

COMPARISON OF DIFFERENT KALMAN FILTERS FOR APPLICATION  
TO MOBILE ROBOTICS

by

Suraj Ravichandran

A Thesis

Submitted to the

Graduate Faculty

of

George Mason University

In Partial fulfillment of

The Requirements for the Degree

of

Master of Science

Electrical Engineering

Committee:



Dr. Gerald Cook, Thesis Director



Dr. Janos Gertler, Committee Member



Dr. Jill K. Nelson, Committee Member



Dr. Andre Manitius, Chairman, Department  
of Electrical & Computer Engineering



Dr. Kenneth S. Ball, Dean, Volgenau School  
of Engineering

Date: \_\_\_\_\_

Spring Semester 2011  
George Mason University  
Fairfax, VA

Comparison of Different Kalman Filters for Application  
to Mobile Robotics

A thesis submitted in partial fulfillment of the requirements for the degree of  
Master of Science at George Mason University

By

Suraj Ravichandran  
Bachelor of Engineering  
Mumbai University, 2011

Director: Dr. Gerald Cook, Professor  
Department of Electrical & Computer Engineering

Spring Semester 2014  
George Mason University  
Fairfax, VA

## Acknowledgments

I am forever in debt of Dr. Cook, without whose support neither would I have come up with this topic, let alone have known about its existence in the first place. Thank you for bearing with me, and for believing that I would FINALLY finish my thesis. Without you to guide me, I would be just another masters student who would have ended up regretting taking up this endeavor of Graduate School. . .

A special thanks to Dr. Janos Gertler, who empathised with my situation and took the time to painstakingly find even the minute mistakes/typos in my thesis, even during the holidays. Your comments and suggestions rendered have given my thesis a professional and technical edge.

It was Dr Jill Nelson's ingenious idea of taking up special registration, which allowed me to defend my thesis an entire semester earlier. I owe you the time I saved as well as the peace of mind that I could only afford because of the special registration option. I also appreciate you agreeing to be on my committee on such short notice and bailing me out of trouble once more.

And finally, any research without proper documentation and administrative protocol is meaningless. Without the help of Patricia Sahs and Jammie Chang I would have been running from pillar to post clueless trying to comprehend what paperwork is needed and what are the deadlines. They have been most helpful and co-operative in my time of need. I am in debt of both of you for all the assistance and guidance that you provided, like the foundation of a building providing constant support whilst staying out of the limelight.

# Table of Contents

	Page
List of Tables . . . . .	vi
List of Figures . . . . .	vii
List of Abbreviations . . . . .	viii
Abstract . . . . .	ix
1 Introduction . . . . .	1
1.1 Limitations of the Linear Kalman Filter . . . . .	1
1.1.1 An Initial yet robust fix – The Extended Kalman Filter . . . . .	2
1.2 The Ultimate Solution – Particle Filter . . . . .	4
1.2.1 Trouble in Paradise – Computationally Prohibitive . . . . .	5
1.3 Why stick to the Kalman Filter? . . . . .	5
1.3.1 Kalman Filter Derivatives . . . . .	6
2 Mobile Robot Dynamics . . . . .	7
2.1 Mobile Robot Setup . . . . .	7
2.1.1 Robot Kinematics in Local Coordinates . . . . .	8
2.1.2 Rotation to Earth Coordinates . . . . .	10
2.2 Steering Control Law . . . . .	10
2.3 Choice of Method for Numerical Integration . . . . .	11
2.3.1 Euler’s Method . . . . .	11
2.3.2 Runge Kutta . . . . .	13
2.4 Sensors . . . . .	14
3 State Estimation using the EKF . . . . .	15
3.1 EKF Derivation for Mobile Robot . . . . .	15
3.1.1 The Final State Space Representation . . . . .	18
3.1.2 Final Flow Algorithm for the EKF . . . . .	20
3.2 EKF Derivatives . . . . .	21
3.2.1 The Iterated Extended Kalman Filter . . . . .	21
3.3 A look on Statistical Linearization Methods for the Non-Linear Kalman Filter . . . . .	23
3.3.1 The Achilles heel of this Approach! . . . . .	24
3.3.2 Monte-Carlo Kalman Filter . . . . .	24

4	State Estimation using the UKF . . . . .	28
4.1	Introduction to the Sigma Point Approach . . . . .	28
4.2	The Unscented Transform . . . . .	30
4.3	The Scaled Unscented Transform . . . . .	31
4.4	Tuning the Weights . . . . .	33
4.5	The UKF Algorithm . . . . .	34
4.5.1	Augmented UKF . . . . .	34
4.5.2	Non-augmented UKF . . . . .	38
4.6	The Square Root UKF . . . . .	38
4.6.1	The SR-UKF Filter Algorithm . . . . .	40
4.7	An Illustrative comparison of the UKF with the EKF . . . . .	43
5	Results: Simulation and Analysis . . . . .	45
5.1	Matlab Simulation . . . . .	45
5.1.1	Environment Variables . . . . .	46
5.2	Graphs . . . . .	48
5.2.1	EKF Path 1 . . . . .	49
5.2.2	EKF Path 2 . . . . .	50
5.2.3	IEKF Path 1 . . . . .	51
5.2.4	IEKF Path 2 . . . . .	52
5.2.5	UKF Path 1 . . . . .	53
5.2.6	UKF Path 2 . . . . .	54
5.2.7	Accuracy and Computational Costs (Time) . . . . .	55
5.3	Verification of the UKF Implementation . . . . .	56
5.3.1	Testing the Unscented Transform . . . . .	56
5.4	Averaging over multiple runs . . . . .	62
5.5	Inference . . . . .	63
5.6	Future Scope . . . . .	63
	Bibliography . . . . .	65

## List of Tables

Table		Page
5.1	Comparison Table for Path 1 . . . . .	55
5.2	Comparison Table for Path 2 . . . . .	56
5.3	EKF v/s UKF MSE averaged over 1000 runs . . . . .	63

## List of Figures

Figure	Page
2.1 Front-Wheel steered robot schematic diagram[5] . . . . .	8
3.1 EKF Process Flow Diagram . . . . .	20
4.1 The transformation of sigma points through a nonlinear function[8] . . . . .	29
4.2 Comparison of mean and covariance sampling by Monte-Carlo Sampling, EKF and UKF[11] . . . . .	44
5.1 EKF Plot for True v/s Estimated Robot Trajectory . . . . .	49
5.2 EKF Plot for True v/s Estimated Heading Angle . . . . .	49
5.3 EKF Plot for True v/s Estimated Robot Trajectory . . . . .	50
5.4 EKF Plot for True v/s Estimated heading Angle . . . . .	50
5.5 IEKF Plot for True v/s Estimated Robot Trajectory . . . . .	51
5.6 IEKF Plot for True v/s Estimated Heading Angle . . . . .	51
5.7 IEKF Plot for True v/s Estimated Robot Trajectory . . . . .	52
5.8 IEKF Plot for True v/s Estimated heading Angle . . . . .	52
5.9 UKF Plot for True v/s Estimated Robot Trajectory . . . . .	53
5.10 UKF Plot for True v/s Estimated Heading Angle . . . . .	53
5.11 UKF Plot for True v/s Estimated Robot Trajectory . . . . .	54
5.12 UKF Plot for True v/s Estimated heading Angle . . . . .	54
5.13 Error Covariance Ellipsoid: Sigma points around the mean with $\alpha = 0.5$ . .	60
5.14 Error Covariance Ellipsoid: Sigma points around the mean with $\alpha = 0.9$ . .	61

## List of Abbreviations

<b>EKF</b>	<b>Extended Kalman Filter</b>
<b>IEKF</b>	<b>Iterated Extended Kalman Filter</b>
<b>UKF</b>	<b>Unscented Kalman Filter</b>
<b>PDF</b>	<b>Probability Density Function</b>
<b>MSE</b>	<b>Mean Squared Error</b>
<b>MCKF</b>	<b>Monte-Carlo Kalman Filter</b>
<b>SR-UKF</b>	<b>Square-Root Unscented Kalman Filter</b>
<b>RK</b>	<b>Runge Kutta</b>



# Abstract

## COMPARISON OF DIFFERENT KALMAN FILTERS FOR APPLICATION TO MOBILE ROBOTICS

Suraj Ravichandran, MS

George Mason University, 2014

Thesis Director: Dr. Gerald Cook

The problem of state estimation of the mobile robot's trajectory being a nonlinear one, the intent of this thesis is to go beyond the realm of the basic Extended Kalman Filter(EKF) and study the more recent nonlinear Kalman Filters for their application to the problem at hand. The various filters that I employ in this study are:

- Extended Kalman Filter(EKF)
- Iterated Extended Kalman Filter (IEKF)
- Unscented Kalman Filter(UKF) and its various forms and alternate editions

The Robot is given different trajectories to run on and the performance of the filters on each of these trajectories is observed. The intensity of process noise and measurement noise are also varied and the effect they have on the estimates studied.

The study also provides a comparison of the computational costs involved in each of the filters above. Pre-established numerically efficient and stable techniques to lower the computational costs of the UKF are employed and their performance in accuracy and computational time is observed and noted.

The UKF is proven to be a better filter in terms of accuracy for the non-linear cases such as inertial navigation systems, but this thesis tests specifically for the system dynamics of the Mobile Robot. The results that are obtained are quite contrasting to the otherwise belief that the UKF should give better accuracy.

## Chapter 1: Introduction

In 1960, Rudolf Kalman proposed the Kalman Filter[1] and completely revolutionized linear filtering. Before I deliver the central idea of my thesis here is a little background into the Kalman Filter.

The Kalman filter is a set of mathematical equations that provides an efficient computational (recursive) means to estimate the state of a process, in a way that minimizes the mean of the squared error. The filter is very powerful in several aspects: it supports estimations of past, present, and even future states, and it can do so even when the precise nature of the modeled system is unknown.[2]

The premise of my thesis centers around the fact that the original Kalman Filter while truly optimal for use with Linear Systems is incapable of dealing with non-linear systems. This is tolerated in the realm of linear dynamics, but, when we analyze most of the real world practical problems, for which we want control and tracking solutions, we realize that most of these cases (if not all) are non-linear in nature. Thus, Electrical Engineering delved into major research and study to tackle these issues.

I propose the application of some of the existing non-linear Kalman Filters to the field of Mobile Robotics, and study their results. This thesis presents an accurate comparison of the various methods that are employed for Mobile Robot State Estimation and an analysis of the same. The aim is to contribute to the ongoing field of Mobile Robotics by sharing my findings.

### 1.1 Limitations of the Linear Kalman Filter

The Linear Kalman Filter has two main problems:

- Linear assumption of system
- Gaussian assumption of Random Variable Probability Distribution

The first limitation is because of the following line of reasoning: The non-linear function of the expectation of a Random Variable is generally not the same as the expectation of the non-linear function of the Random Variable. The equation below delineates it in mathematical form.

$$E \{f(x)\} \neq f(E \{x\}) \tag{1.1.1}$$

where  $f(\cdot)$  is a non-linear function.

This non-equality is not present for linear functions as the following is true for a linear function.

$$E \{g(x)\} = g(E \{x\})$$

where  $g(\cdot)$  is a linear function.

The second limitation is more inherent in the nature of the Kalman Filter. The reason for this is that it assumes all of its distributions i.e, the measurement noise, the process disturbance and the main state variable being estimated to be Gaussian. This has its benefits since it allows the Kalman Filter to be broken down to linear algebraic steps; thus making it mathematically elegant and computationally efficient. However, it places an important limitation on its uses in the practical world of problems.

### 1.1.1 An Initial yet robust fix – The Extended Kalman Filter

With the increasing need to apply Kalman Filters to the non-linear domain, the engineering community came up with an ingenious solution. The Extended Kalman Filter overcomes the problem faced by the linearity limitation (1.1.1), by just linearizing the non-linear function about its first order Taylor series expansion. It can be summarized in the following explanation.[3]

Consider the following non-linear state dynamic equations ...

$$\dot{x}(t) = f(x(t), t) + w(t) \quad (1.1.2a)$$

$$z(t) = h(x(t), t) + v(t) \quad (1.1.2b)$$

where  $w(t)$  is the process disturbance and  $v(t)$  is the measurement noise. Both are assumed to be zero-mean Gaussian process i.e.

$$E \{v(t)\} = E \{w(t)\} = 0$$

If the non-linear function  $f(x(t))$  is differentiable, then it can be linearized about the estimated trajectory  $\hat{x}(t)$  as follows:

$$\begin{aligned} f(x(t), t) &= f(\hat{x}(t), t) + \left( \frac{\partial f(x(t), t)}{\partial x(t)} \Big|_{x(t)=\hat{x}(t)} \right) (x(t) - \hat{x}(t)) \\ &+ \frac{1}{2} \left( \frac{\partial^2 f(x(t), t)}{\partial^2 x(t)} \Big|_{x(t)=\hat{x}(t)} \right) (x(t) - \hat{x}(t))^2 \\ &\quad + \text{higher order terms} \dots \end{aligned} \quad (1.1.3)$$

The key fact that enables the working of the Extended Kalman filter is that, since we deal with non-linear yet almost linear dynamics the quadratic and higher order terms of (1.1.3) can be neglected. This would yield the following perturbation about the estimated trajectory  $\delta\hat{x}$ :

$$\delta\dot{x}(t) = f(\hat{x}(t), t) + \left( \frac{\partial f(x(t), t)}{\partial x(t)} \Big|_{x(t)=\hat{x}(t)} \right) \delta x(t) \quad (1.1.4)$$

We can now replace the 'F(t)' matrix of the fundamental equation with the following Jacobian  $F_j$ :

$$F_j = \frac{\partial f(x(t), t)}{\partial x(t)} \Big|_{x(t)=\hat{x}(t)}$$

$$F_j = \left[ \begin{array}{ccccc} \frac{\partial f_1}{\partial x_1} & \frac{\partial f_1}{\partial x_2} & \frac{\partial f_1}{\partial x_3} & \dots & \frac{\partial f_1}{\partial x_n} \\ \frac{\partial f_2}{\partial x_1} & \frac{\partial f_2}{\partial x_2} & \frac{\partial f_2}{\partial x_3} & \dots & \frac{\partial f_2}{\partial x_n} \\ \vdots & \vdots & \vdots & \ddots & \vdots \\ \frac{\partial f_n}{\partial x_1} & \frac{\partial f_n}{\partial x_2} & \frac{\partial f_n}{\partial x_3} & \dots & \frac{\partial f_n}{\partial x_n} \end{array} \right]_{x(t)=\hat{x}(t)} \quad (1.1.5)$$

Similarly the Jacobian for the Observer Matrix H can be given as  $H_j$

$$H_j = \left[ \begin{array}{ccccc} \frac{\partial h_1}{\partial x_1} & \frac{\partial h_1}{\partial x_2} & \frac{\partial h_1}{\partial x_3} & \dots & \frac{\partial h_1}{\partial x_n} \\ \frac{\partial h_2}{\partial x_1} & \frac{\partial h_2}{\partial x_2} & \frac{\partial h_2}{\partial x_3} & \dots & \frac{\partial h_2}{\partial x_n} \\ \vdots & \vdots & \vdots & \ddots & \vdots \\ \frac{\partial h_n}{\partial x_1} & \frac{\partial h_n}{\partial x_2} & \frac{\partial h_n}{\partial x_3} & \dots & \frac{\partial h_n}{\partial x_n} \end{array} \right]_{x(t)=\hat{x}(t)} \quad (1.1.6)$$

With the exception of the state forward propagation step, we replace the matrices of F and H in the equations of the Original Kalman Filter[1] with the Jacobians  $F_j$  and  $H_j$  respectively. The state propagation step remains the same complete nonlinear function  $f(x)$ .

## 1.2 The Ultimate Solution – Particle Filter

The Particle filter overcomes both limitations that are faced by the Kalman Filter i.e Assumption of Linearity as well as the Gaussian Nature of the Probability Distribution Function. Particle filters or Sequential Monte Carlo (SMC) methods are a set of on-line posterior density estimation algorithms that estimate the posterior density of the state-space by directly implementing the Bayesian recursion equations. SMC methods use a grid-based approach, and use a set of particles to represent the posterior density. These filtering methods make no restrictive assumption about the dynamics of the state-space or the density function. SMC methods provide a well-established methodology for generating samples

from the required distribution without requiring assumptions about the state-space model or the state distributions. The state-space model can be non-linear and the initial state and noise distributions can take any form required.[4]

### **1.2.1 Trouble in Paradise – Computationally Prohibitive**

The accuracy of the particle filter relies on the number of samples (particle) it uses. It requires a very large number of particles to produce a decent estimate and an even larger set to overcome the EKF in results. While it does overcome the EKF and by a good amount, the simultaneous propagation of all these particles in real-time puts a heavy load on the computation part of the scheme. Thus, it levies a time constraint in a practical scenario where extraordinary computational power is not available for filtering and tracking. Thus, it renders itself to be very slow and cannot keep up in real time with estimation process. This problem only scales up with higher dimensionality of the system dynamics. Thus, unless one has a super computer to spare for this, the Particle Filter becomes somewhat a lesser desired alternative.

## **1.3 Why stick to the Kalman Filter?**

Most of the Control problems that are currently being faced are non-linear, but the extent of their non-linearity is not high. They are only non-linear within reasonable boundaries. This type of problems can be efficiently tackled by the derivatives of the Kalman Filter. Plus, although its prime Gaussian Assumption is not always correct, it does render its equations to be represented in state space matrix form, which reduces the math to being elegant. One can now rely on matrix math to simplify the equations and also make them computationally efficient. In addition, most of the Mobile Robot States can be accurately modeled via a Gaussian distribution with little to negligible error in performance. Thus, the Kalman Filter is a good choice not only in theory but also in practice as it does the job just a couple of notches below the optimal solution and is computationally super efficient.

### 1.3.1 Kalman Filter Derivatives

Following our current discussion on why to stick with the Kalman Filter, there are a lot of developments in the non-linear Kalman Filtering field. These were made with a sole objective in mind: To Augment the Performance of the Extended Kalman Filter and improve the scope for non-linear tracking and filtering.

I explore some of these derivatives in this thesis. These derivatives stick to the Gaussian assumption of the Kalman Filter, but modify some of the steps of the algorithm to be more non-linear application specific. Thus, these derivatives help us to remain with the Kalman Filter and enjoy its computational efficiency while trying to improve its performance and accuracy for non-linear systems.

The various Non-Linear Kalman Filters (Derivatives) that I employ are:

1. Extended Kalman Filter (EKF)
2. Iterated Extended Kalman Filter (IEKF)
3. Unscented Kalman Filter (UKF)



## Chapter 2: Mobile Robot Dynamics

### 2.1 Mobile Robot Setup

For my thesis, I employ a front-wheel steered robot to perform all the filtering and tracking experiments on. The reason for this is that, even though the differential drive mobile robot has some distinct maneuverability advantages, it faces some serious practical terrain constraints. For example, on a carpet or a surface similar to a carpet, the differential drive robot will not be able to make turns effectively due to the surface characteristics. Plus even in the real life scenario of driving a car, most of us drive a 2 wheel drive vehicle, which in essence is a front-wheel steered mechanism. Thus, I choose this type of robot instead of anything else.

In the front-wheel steered robot, only the rear wheels are powered and the front wheels provide the robot direction. One can steer the robot in the desired direction by means of an actuator.

### 2.1.1 Robot Kinematics in Local Coordinates

The diagram below will help us get a better sense of the underlying mechanism behind the front-wheel steered robot.

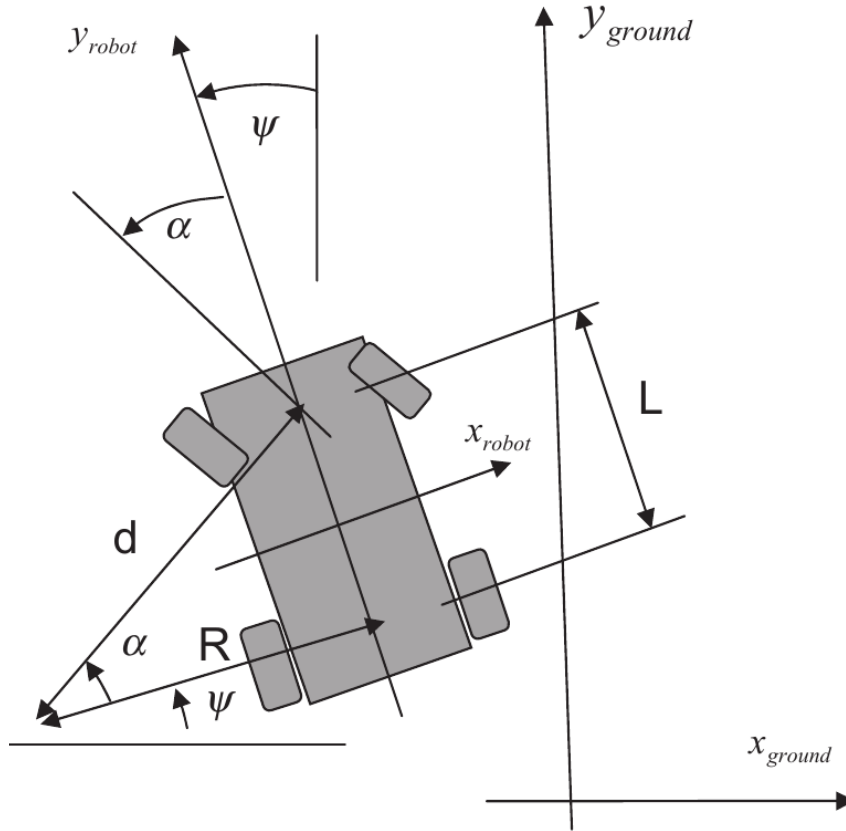


FIGURE 2.1: Front-Wheel steered robot schematic diagram[5]

Keeping this figure as our reference we go ahead and start deriving the kinematic equations of motion for our mobile robot.<sup>1</sup>

In reality when the two front wheels of the robot make a different angle each with respect to the longitudinal axis of the robot,  $y_{robot}$  to avoid slippage and attain stability. However, to simplify things a bit for our simulation (since our major objective is comparison of filters and not precision modelling of the mobile robot), we consider the angle that the midpoint of the

<sup>1</sup>This figure 2.1 and the consequent equations derived are taken from the book – Mobile Robotics:Nav, Control and Rem. Sensing[5] if the reader wants an in-depth review of the same he can refer chapter 1 in the mentioned book.

front wheels (midpoint of the line that joins the two front wheels together) w.r.t  $y_{robot}$  to be defined as  $\alpha$ , measured in the counter-clockwise direction. The angle that the longitudinal axis,  $y_{robot}$ , makes with respect to the  $y_{ground}$  axis is defined as  $\psi$ , also measured in the counter-clockwise direction. The instantaneous center about which the robot is turning is the point of intersection of the two lines passing through the wheel axes. The velocity of the rear wheels is termed as  $v_{rearwheel}$ <sup>2</sup>.

From the geometry we have,

$$\frac{L}{R} = \tan \alpha$$

which may be solved to yield the instantaneous radius of curvature for the path of the midpoint of the rear axle of the robot.

$$R = \frac{L}{\tan \alpha} \tag{2.1.1}$$

From the geometry we also have

$$v_{rearwheel} = R \frac{d}{dt}(\psi) = R\dot{\psi}$$

re-arranging, we get,

$$\dot{\psi} = \frac{v_{rearwheel}}{R}$$

Now if substitute equation (2.1.1) in this, we get,

$$\dot{\psi} = \frac{v_{rearwheel}}{L/\tan \alpha} = \frac{v_{rearwheel}}{L} \tan \alpha \tag{2.1.2}$$

The final set of kinematic equations of motion in the robot (local) coordinate frame are as

---

<sup>2</sup>Even  $v_{rearwheel}$  is different for each of the two rear wheels of the robot as they each turn with the same center of curvature but a different radius of curvature. Again for the sake of simplicity we take the average velocity of the midpoint of these two rear wheels and carry on with our simulation

follows:

$$v_x = 0 \quad (2.1.3a)$$

$$v_y = v_{rearwheel} \quad (2.1.3b)$$

$$\dot{\psi} = \frac{v_{rearwheel}}{L} \tan \alpha \quad (2.1.3c)$$

### 2.1.2 Rotation to Earth Coordinates

The equations described in (2.1.3) are in local coordinate space of the mobile robot. However, for state estimation and other purposes, like reaching a target or rendezvous with another vehicle, we require the knowledge of the kinematic equations of motion in the global earth coordinate frame. For this, we need to rotate the equations through the required rotation matrices, given the orientation angles and position of the robot itself with respect to the earth frame. After doing these transformations, we get the final equations of motion as follows:-

$$\dot{x}(t) = -v_{rearwheel} \sin \psi(t) \quad (2.1.4a)$$

$$\dot{y}(t) = v_{rearwheel} \cos \psi(t) \quad (2.1.4b)$$

$$\dot{\psi}(t) = \frac{v_{rearwheel}}{L} \tan \alpha(t) \quad (2.1.4c)$$

## 2.2 Steering Control Law

We use the following proportional control law for our front-wheel steering.

$$\alpha(t) = \begin{cases} Gain * (\psi_{des}(t) - \psi(t)) & \text{if } abs(Gain * (\psi_{des}(t) - \psi(t))) \leq \pi/4 \\ \frac{\pi}{4} sgn(\psi_{des}(t) - \psi(t)) & \text{if } abs(Gain * (\psi_{des}(t) - \psi(t))) > \pi/4 \end{cases} \quad (2.2.1)$$

In the above equation  $\psi_{des}$  stands for heading desired i.e. the desired heading that we want the robot to undertake and  $\psi$  is the current heading of the robot. We calculate desired heading at each point in time, by using the final destination coordinates  $(x_{des}, y_{des})$  and the current time instant robot coordinates in earth frame(x,y). The equation for the desired heading is given as follows:

$$\psi_{des}(t) = -\tan^{-1} \left( \frac{x_{des}(t) - x(t)}{y_{des}(t) - y(t)} \right) \quad (2.2.2)$$

Note that while the desired destination coordinates are written as time dependent variables  $(x_{des}(t), y_{des}(t))$ , they can also be constant throughout i.e we also have just a single destination to go to.

The *Gain* affects the rate at which the robot can turn. It can only be modulated within a specific range after which the robot steering enters saturation, as from equation (2.2.1), it is evident that  $|\pi/4|$  is the maximum allowable steering angle that  $\alpha$  can take. Extending this value would result in a very impractical design of the front wheel steering.

## 2.3 Choice of Method for Numerical Integration

The equations described in (2.1.4) are in continuous time and we need to be expressed in discrete time in order for our Kalman Filters to run on any computing devices. There are several methods of numerical integration that one could employ for the non-linear equations at hand, but I have employed only two of the significant ones: Euler's Method and the Runge Kutta method.

### 2.3.1 Euler's Method

The Euler's Method for Numerical Integration is a first-order Taylor series approximation to integration. The gist of it is that the derivative may be approximated by a finite difference.

Employing this to our existing  $\dot{x}$  equation, we get,

$$\dot{x}(t) = \frac{x(t + \Delta t) - x(t)}{\Delta t}$$

Where  $\Delta t$  is just a small increment in time, thus re-arranging this we get,

$$x(t + \Delta t) \approx x(t) + \dot{x}(t)\Delta t \tag{2.3.1}$$

Setting the discrete time sampling interval as  $\Delta t = \delta t$  and the time  $t = k\delta t$ , where  $k$  is the iteration number i.e the  $k^{th}$  iteration. Then we proceed to apply the discretization scheme from the above equation (2.3.1) to our robot kinematic equations of motion mentioned in (2.1.4), we get the following results,

$$x((k + 1)\delta t) = x(k\delta t) - \delta t * v_{rearwheel} \sin \psi(k\delta t)$$

$$y((k + 1)\delta t) = y(k\delta t) + \delta t * v_{rearwheel} \cos \psi(k\delta t)$$

$$\psi((k + 1)\delta t) = \psi(k\delta t) + \delta t * \frac{v_{rearwheel}}{L} \tan \alpha(k\delta t)$$

The above equations can be a bit cumbersome, thus from now on we will make use of the following style of expressing discrete time equations in general, let alone the kinematic equations,

$$\mathbf{x}_{k+1} = \mathbf{x}_k - \delta t * v_{rearwheel} \mathbf{sin} \psi_k \tag{2.3.2a}$$

$$\mathbf{y}_{k+1} = \mathbf{y}_k + \delta t * v_{rearwheel} \mathbf{cos} \psi_k \tag{2.3.2b}$$

$$\psi_{k+1} = \psi_k + \delta t * \frac{v_{rearwheel}}{L} \mathbf{tan} \alpha_k \tag{2.3.2c}$$

I removed the time dependence of  $v_{rearwheel}$  on  $k\delta t$ , as for our simulations and analysis we keep  $v_{rearwheel}$  constant throughout the trajectory of the mobile robot.

### 2.3.2 Runge Kutta

There are a family of Runge Kutta methods for numerical integration, however the one we will be discussing here is called as the Runge Kutta 4 a.k.a RK4. This method is sometimes referred to as the classical RK Method. The RK method is generally more accurate than the Euler's Method.

The concept of it is as follows . . . Consider the initial value problem:

$$\dot{x} = f(t, x(t))$$

$$x(t_0) = x_0$$

Here,  $x$  is an unknown function (scalar or vector) of time  $t$  which we would like to approximate; we are told that  $\dot{x}$ , the rate at which  $x$  changes, is a function of  $t$  and of  $x$  itself. At the initial time  $t_0$  the corresponding  $x$ -value is  $x_0$ . The function  $f$  and the data  $t_0, x_0$  are given.

Now we choose a sampling interval, which is greater than 0 to be as  $\delta t = h$ .

$$x_{n+1} = x_n + \frac{1}{6}h (k_1 + 2k_2 + 2k_3 + k_4) \tag{2.3.3a}$$

$$t_{n+1} = t_n + h \tag{2.3.3b}$$

for  $n = 0, 1, 2, 3, \dots$ , using

$$k_1 = f(t_n, x_n), \tag{2.3.3c}$$

$$k_2 = f(t_n + \frac{1}{2}h, x_n + \frac{h}{2}k_1), \tag{2.3.3d}$$

$$k_3 = f(t_n + \frac{1}{2}h, x_n + \frac{h}{2}k_2), \tag{2.3.3e}$$

$$k_4 = f(t_n + h, x_n + hk_3). \tag{2.3.3f}$$

Here  $x_{n+1}$  is the RK4 approximation of  $x(t_{n+1})$ , and the next value ( $x_{n+1}$ ) is determined by the present value ( $x_n$ ) plus the weighted average of four increments; each increment is the product of the size of the interval,  $h$ , and an estimated slope specified by function  $f$  on the right-hand side of the differential equation.

## 2.4 Sensors

For Mobile Robot State Estimation and Tracking one can choose from a multitude of sensors such as GPS or Quadrature Encoded Odometry. Here I remain agnostic to the choice and assume that I have two sensors available at my disposal which give direct measurements of the robot's  $x$  and  $y$  coordinates in the earth frame. I take the liberty to assume that all frame rotation and other offset calculations are done at a higher abstraction layer and provided to me. There are no measurements for the heading i.e  $\psi_k$  this makes the Kalman Filter do some extra work, as well as exhibit its potential in cases where one does not have all the measurements available.

Thus my observer function  $\mathbf{h}(\cdot)$  is linear and direct in form.



## Chapter 3: State Estimation using the EKF

### 3.1 EKF Derivation for Mobile Robot

The first step in any filter would be to forward propagate the state. This is also called as the *a priori* prediction. A point to note, all linear filters would have the following equations as a sum of the products of different matrices. One cannot do so in the non-linear case as no linear matrix product can be found for a non-linear function. That being said, we still use the exact non-linear function to propagate the state estimate forward.

$$\hat{X}_{k+1} = f(\hat{X}_k, U_k, w_k)$$

Where:

$\hat{X} \sim$  Entire Estimated State Vector, which in our case is  $\hat{X}_k = \begin{bmatrix} \hat{x}_k \\ \hat{y}_k \\ \hat{\psi}_k \end{bmatrix}$

$U \sim$  Control Input Matrix/Vector, which in our case is just a single scalar  $\alpha$

$w \sim$  This is the process disturbance

Now as discussed in section 1.1.1 on page 4, we need to first find the jacobians for the F and H matrices to carry on with the Extend Kalman Filter Algorithm.

First, lets derive the Jacobian for the F matrix i.e.  $F_j$ . For this we need to substitute equation (2.3.2) in the equation (1.1.5). The steps involved for taking the partial differentials and forming the Jacobian are given as follows:

Velocity of the rear wheel is denoted as just  $v$  instead of  $v_{rearwheel}$ <sup>1</sup>.

$$\begin{aligned}
F_j &= \left. \frac{\partial f(X_k)}{\partial x(t)} \right|_{X=\hat{X}_k} \\
&= \left. \begin{bmatrix} \frac{\partial f_1}{\partial x_1} & \frac{\partial f_1}{\partial x_2} & \frac{\partial f_1}{\partial x_3} \\ \frac{\partial f_2}{\partial x_1} & \frac{\partial f_2}{\partial x_2} & \frac{\partial f_2}{\partial x_3} \\ \frac{\partial f_n}{\partial x_1} & \frac{\partial f_n}{\partial x_2} & \frac{\partial f_n}{\partial x_3} \end{bmatrix} \right|_{X=\hat{X}_k} \\
&= \begin{bmatrix} \frac{\partial}{\partial x} (x_k - \delta t \cdot v \sin \psi_k) & \frac{\partial}{\partial y} (x_k - \delta t \cdot v \sin \psi_k) & \frac{\partial}{\partial \psi} (x_k - \delta t \cdot v \sin \psi_k) \\ \frac{\partial}{\partial x} (y_k + \delta t \cdot v \cos \psi_k) & \frac{\partial}{\partial y} (y_k + \delta t \cdot v \cos \psi_k) & \frac{\partial}{\partial \psi} (y_k + \delta t \cdot v \cos \psi_k) \\ \frac{\partial}{\partial x} (\psi_k + \delta t \cdot \frac{v}{L} \tan \alpha_k) & \frac{\partial}{\partial y} (\psi_k + \delta t \cdot \frac{v}{L} \tan \alpha_k) & \frac{\partial}{\partial \psi} (\psi_k + \delta t \cdot \frac{v}{L} \tan \alpha_k) \end{bmatrix} \quad (3.1.1) \\
&= \begin{bmatrix} 1 & 0 & -\delta t \cdot v \cos \psi_k \\ 0 & 1 & -\delta t \cdot v \sin \psi_k \\ 0 & 0 & 1 \end{bmatrix} \\
&= \underbrace{\begin{bmatrix} 1 & 0 & 0 \\ 0 & 1 & 0 \\ 0 & 0 & 1 \end{bmatrix}}_{I_{3 \times 3}} + \delta t \begin{bmatrix} 0 & 0 & -v \cos \psi_k \\ 0 & 0 & -v \sin \psi_k \\ 0 & 0 & 0 \end{bmatrix}
\end{aligned}$$

In the case on the linear Kalman Filter, we would have a co-efficient matrix that multiplies with the control input (this is usually denoted by the matrix 'G'). In the non-linear case the control input is integrated into the state propagation equation within the non-linear function and cannot be separated and written as the product of the co-efficient matrix and the raw control input. However, we do still need the Jacobian of the G matrix for other EKF equations. Thus, we derive it in the same manner as we did the for  $F_j$ . Except this time instead of differentiating it with respect to the state vector  $X_k$  we differentiate it with

---

<sup>1</sup>I do this in the derivation to save space and make the Jacobians appear much more compact

respect to the control input  $\alpha$ .

$$\begin{aligned}
 G_j &= \left. \frac{\partial f(X_k)}{\partial \alpha} \right|_{\alpha_k} \\
 &= \left. \begin{bmatrix} \frac{\partial f_1}{\partial \alpha} \\ \frac{\partial f_2}{\partial \alpha} \\ \frac{\partial f_3}{\partial \alpha} \end{bmatrix} \right|_{\alpha_k} \\
 &= \begin{bmatrix} \frac{\partial}{\partial \alpha} (x_k - \delta t \cdot v \sin \psi_k) \\ \frac{\partial}{\partial \alpha} (y_k + \delta t \cdot v \cos \psi_k) \\ \frac{\partial}{\partial \alpha} (\psi_k + \delta t \cdot \frac{v}{L} \tan \alpha_k) \end{bmatrix} \\
 &= \delta t \begin{bmatrix} 0 \\ 0 \\ \frac{v}{L} \left( \frac{1}{\cos^2 \alpha} \right) \end{bmatrix}
 \end{aligned}$$

Now, as already discussed I have direct measurements for the first two elements of the state vector, the observation matrix H is linear and we do not to derive the Jacobian. Therefore, this is the form of our H-Matrix:

$$H = \begin{bmatrix} 1 & 0 & 0 \\ 0 & 1 & 0 \end{bmatrix}$$

Now, before we move on to the State Space Representations of the EKF, I would like to state the various initial conditions that are used for the purpose of my simulations. The

initial error propagation  $P_0$  is given by the following formula:

$$P_0 = \mathbf{E}[(X_0 - \hat{X}_0)(X_0 - \hat{X}_0)^T]$$

Since we usually have neither the initial State of the Robot nor information about its Probability Distribution Function(PDF), we resort to trial and error methods, and this is what is specifically used

$$P_0 = \begin{bmatrix} 0.2^2 & 0 & 0 \\ 0 & 0.2^2 & 0 \\ 0 & 0 & \left(\frac{\pi}{4.0}\right)^2 \end{bmatrix} \quad (3.1.2)$$

The rest of the initial conditions and constants are specified in detail in the Simulation and Analysis Chapter.

### 3.1.1 The Final State Space Representation

The exact equation for forward propagation of the main state vector  $\hat{X}$  is given by

$$\hat{X}(-)_{k+1} = \hat{X}(+)_{k} + \delta t \begin{bmatrix} 0 & 0 & -v \cos \psi_k \\ 0 & 0 & -v \sin \psi_k \\ 0 & 0 & 0 \end{bmatrix} \quad (3.1.3a)$$

This is also called as the *a priori* estimate of state or just as 'prediction', this is why we denote it with a (-) symbol.<sup>2</sup>

The next step would be to generate the *a priori* version of the Error Covariance Matrix. It is denoted as  $P(-)$

$$P(-)_{k+1} = F_j P(+)_k F_j^T + G_j Q_k G_j^T \quad (3.1.3b)$$

This step is also referred to as the Error Covariance Propagation Step, and if  $k=1$  then we replace the  $P(+)_k$  with  $P_0$ . The  $Q$  matrix mentioned here is the covariance of the process disturbance  $w_k$  and is given by

$$Q = \mathbf{E}[w_k w_k^T]$$

Now calculating the Kalman Gain  $K$ ,

$$K = P(-)_{k+1} H^T [H P(-)_{k+1} H^T + R_k]^{-1} \quad (3.1.3c)$$

Where  $R$  is the Covariance of the measurement noise  $v_k$  and is given by

$$R_k = \mathbf{E}[v_k v_k^T]$$

At this point in our algorithm we receive the measurement update from the sensors for the  $(k+1)^{th}$  iteration i.e.  $Y_{k+1}$  and so we can now update our beliefs accordingly. So first, we add the 'Innovation' to the State Prediction  $\hat{X}(-)_{k+1}$

$$\hat{X}(+)_{k+1} = \hat{X}(-)_{k+1} + K_k [Y_{k+1} - H \hat{X}(-)_{k+1}] \quad (3.1.3d)$$

This is also called as the *posteriori* estimate, hence the  $(+)$  sign.

Finally, we are left with updating the Error Covariance to include the data from the recent measurement update, we call this  $P(+)$ , the plus sign is for the *a posteriori* belief update.

$$P(+)_k = [I_{n \times n} - KH] P(-)_k [I_{n \times n} - KH]^T + KRK^T \quad (3.1.3e)$$

The above equation is called the "Joseph's Form" of the covariance update equation and is used in cases when there might exist computational round-off errors or the Kalman Gain  $K$  is sub-optimal. The 'n' represents the dimensionality of the state vector  $\hat{X}$  and in our case  $n=3$ .

Once we are done with all the above steps we go back to the first step, increment  $k$  and start the entire cycle again.

### 3.1.2 Final Flow Algorithm for the EKF

The above derivation can be summed up as a flow diagram which can capture the entire essence of the EKF.

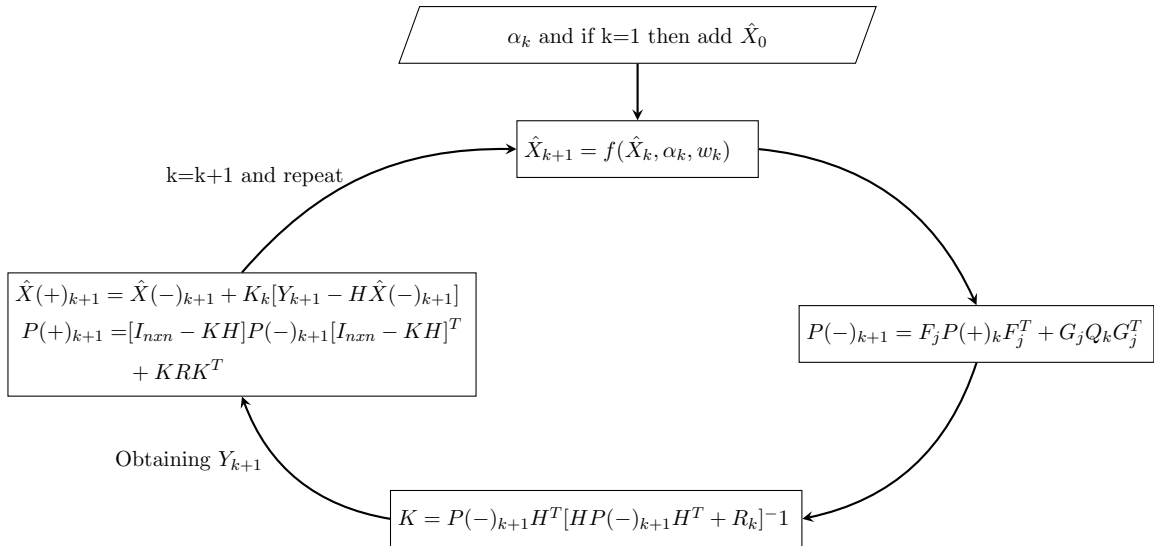


FIGURE 3.1: EKF Process Flow Diagram

## 3.2 EKF Derivatives

There have been a number of derivatives that have evolved out of the EKF. Some employed Square Root Filtering techniques for the error covariance matrix  $P$ , while others resorted to techniques like using Neural Networks and Fuzzy Logic to train the EKF to perform better over the available data. There also have been some very simple yet effective derivatives which relied on exploiting the higher order terms of the Taylor Series Expansion (1.1.3) to improve the accuracy of the EKF. They did so by including more than just the 1<sup>st</sup> term of the Taylor series expansion for approximating the non-linear state functions. Such filters are termed as Higher Order EKFs. The one that I employ for the Mobile Robot State Estimation is the Iterated Extended Kalman Filter. We discuss its concept and the algorithmic modifications that it makes to the EKF below.

### 3.2.1 The Iterated Extended Kalman Filter

There are many ways of approaching the Taylor series expansion scheme to increase the accuracy of the EKF. One method of accomplishing this, is to write the estimate  $\hat{X}(+)_{k+1}$  in a higher-order power series in  $Y_k$ . Another more commonly used approach is to include more terms in the expansions for  $f(\hat{X}_k)$  and  $h(\hat{X}_k)$ . The method that is used in this thesis improves the post measurement (*a posteriori*) State Estimate  $\hat{X}(+)_{k+1}$  by repeatedly calculating  $\hat{X}(+)_{k+1}$ ,  $K_{k+1}$  and  $P(+)_{k+1}$ , each time linearizing about the recent estimate.[6] The EKF linearizes the observer function by partial differentiation (1.1.6), evaluated at the *a priori* estimate

$$H_k = \left. \frac{\partial h}{\partial x} \right|_{X=\hat{X}(-)_k}$$

The IEKF uses successive evaluations of the partial derivatives at better estimates of  $\hat{X}$ ,

starting with the *a posteriori* estimate from the EKF[3]<sup>3</sup>, which is the zeroth iteration.

$$\hat{X}_k^{[0]} = \hat{X}(+)_k \quad (3.2.1)$$

The final *a posteriori* covariance of estimation uncertainty is calculated only after the last iteration, using the final iterated value of H.

The iteration succession is as follows for  $i = 1, 2, 3, \dots$ :

$$H_k^{[i]} = \left. \frac{\partial h}{\partial x} \right|_{X=\hat{X}_k^{[i-1]}} \quad (3.2.2a)$$

$$K_k^{[i]} = P(-)_k H_k^{T[i]} [H_k^{[i]} P(-)_k H_k^{T[i]} + R_k]^{-1} \quad (3.2.2b)$$

$$\tilde{Y}_k^{[i]} = Y_k - h(\hat{X}_k^{[i-1]}) \quad (3.2.2c)$$

$$\hat{X}_k^{[i]} = \hat{X}(-)_k + K_k^{[i]} \tilde{Y}_k^{[i]} - H_k^{[i]} [\hat{X}(-)_k - \hat{X}_k^{[i-1]}] \quad (3.2.2d)$$

We continue the above algorithm repeatedly until some stopping criteria is met. There are a lot of different criteria that one can use, but the one I employ for my simulations is as follows:

$$|[\hat{X}_k^{[i]} - \hat{X}_k^{[i-1]}]^T [\hat{X}_k^{[i]} - \hat{X}_k^{[i-1]}]| < \epsilon_{limit} \quad (3.2.3)$$

Where the threshold  $\epsilon_{limit}$  has been chosen manually and is application specific.

The final estimate now is  $\hat{X}_k^{[i]}$  and the associated *a posteriori* covariance matrix  $P(+)_k$  is obtained by substituting the Kalman Gain  $K_k^{[i]}$  and  $H_k^{[i]}$  obtained above into the covariance update formula (3.1.3e) to get the following result:

$$P(+)_k = [I_{n \times n} - K_k^{[i]} H_k^{[i]}] P(-)_k [I_{n \times n} - K_k^{[i]} H_k^{[i]}]^T + K_k^{[i]} R K_k^{T[i]} \quad (3.2.4)$$

Note: The IEKF Algorithm that I demonstrate above improves the estimate  $\hat{X}(+)_{k+1}$  by

---

<sup>3</sup>The equations for the IEKF have been taken from the following book[3]



linearizing it repeatedly over the function  $h(\cdot)$ . However, earlier I have assumed that my Observation Matrix  $H$  is linear and that I make direct linear measurements, this clashes with the fact that we even need linearization about the  $h(\cdot)$  function. Thus, I wanted to clarify by explaining my reasons for choosing the IEKF in my thesis. In many real life scenarios the sensors for mobile robots are non-linear in nature and we do not have the privileges of the linear  $H$  matrix. Hence, I purposefully give an arbitrary non-linear  $h(\cdot)$  function to my filter, just to gauge the effectiveness of the IEKF in such cases. It must be noted that ONLY for the IEKF analysis and simulations do i change the  $h(\cdot)$  to be non-linear and for the rest of the topics of my thesis it remains as previously discussed, linear.

### 3.3 A look on Statistical Linearization Methods for the Non-Linear Kalman Filter

We have discussed the applications of Taylor Series expansion for the design of the sub-optimal EKF. An alternate approach and one that is generally more accurate is referred to as statistical approximation. The basic principle of this technique is conveniently illustrated for a scalar function,  $s(x)$ , of a RV  $x$ .<sup>[6]</sup><sup>4</sup>

Consider that  $s(x)$  is to be approximated by a series expansion of the form

$$s(x) \simeq n_0 + n_1x + n_2x^2 + \dots + n_mx^m \quad (3.3.1)$$

The problem of determining appropriate coefficients  $n_k$  is similar to the estimation problem where an estimate of a RV is sought from given measurement data. Analogous to the concept of estimation error, we define a function representation error,  $e$ , of the form

$$e = s(x) - n_0 - \dots - n_mx^m$$

---

<sup>4</sup>The example of the statistical linearization method(the analysis and the equations) is taken from the following source[6]

It is desirable that  $n_k$ 's be chosen so that  $e$  is small in some "average" sense; any procedure that is used to accomplish this goal, which is based upon the statistical properties of  $x$ , can be thought of as a statistical approximation technique.

The most frequently used method for choosing the coefficients in (3.3.1) is to minimize the mean square error value of  $e$ . This is achieved by forming

$$\mathbf{E} \left[ (s(x) - n_0 - n_1x - \dots - n_mx^m)^2 \right]$$

and setting the partial derivatives of this quantity with respect to each  $n_k$  equal to zero. The result is a set of algebraic equations, linear in the  $n_k$ 's, that can be solved in terms of the moments and cross-moments of  $x$  and  $s(x)$ . We can now abstractly gauge that statistical approximation has a distinct advantage over the Taylor Series expansion; it does not require the existence of derivatives of  $s(\cdot)$ .

### 3.3.1 The Achilles heel of this Approach!

With all that being said, there is a major drawback that we face in statistical linearization techniques, and that is the expectation operation. This would require knowledge of the probability density function of  $x$  in order to compute the coefficients  $n_k$ . This requirement does not exist for the Taylor Series expansion employed in the EKF.

One may argue that approximations can often be made for the pdf used to calculate the coefficients  $n_k$ , such that the resulting expansion for  $s(x)$  is considerably more accurate than the Taylor series, from a statistical point of view. While, this being true, I do not delve into this topic because the nature of approximate pdfs is complex, and which pdf best suits the approximation purposes is beyond the scope of this thesis.

### 3.3.2 Monte-Carlo Kalman Filter

One such example of a filter that uses statistical linearization techniques is the Monte-Carlo Kalman Filter(MCKF). It draws samples from the prior distribution of  $X_k$  and passes them

through the non-linear state propagation function  $f(X)$ . Now, with these transformed samples, we can draw the *a priori* mean and covariance as follows<sup>[7]</sup><sup>5</sup>:

$$\hat{X}(-)_{k+1} = \frac{1}{N} \sum_{i=1}^N f(X_k^i) \quad (3.3.2)$$

This gives us the mean of the distribution that is propagated forward through the non-linear function  $f$ . Here  $X_k^i$  denotes the samples taken from the *prior* distribution of  $X$ . These points are taken about the principal axis of the pdf. Now, for the covariance,

$$P(-)_{k+1} = Q + \frac{1}{N} \sum_{i=1}^N \left[ (f(X_k^i) - \hat{X}(-)_{k+1})(f(X_k^i) - \hat{X}(-)_{k+1})^T \right] \quad (3.3.3)$$

This gives us the covariance of the distribution (in our case it is the error covariance) that is propagated forward through the non-linear function  $f$ .

Note: Here we first draw samples from the prior distribution, pass it through the non-linear function and then approximate their mean by averaging methods (with the assumption of the law of large numbers in our favour). We could also choose to have propagated the mean of the prior distribution of  $X$  i.e.  $\hat{X}(+)_{k+1}$  through the function, instead of what we are currently doing. This would require that the function  $f$  be linear and the samples perfectly Gaussian. I explained the primary difficulty encountered in the later approach for non-linear functions in equation (1.1.1).

We can continue in a similar fashion and pass the samples through the observer function  $h$  and obtain the mean and covariance of  $\hat{Y}_{k+1}$  as well as the cross covariance of  $\hat{X}$  and  $\hat{Y}$  (which is needed to calculate the Kalman Gain  $K$ ).

$$Y_{k+1}^i = h(f(X_k^i))$$

---

<sup>5</sup>The information for the Monte-Carlo Kalman Filter equations was obtained in the following source [7]

$$\hat{Y}_{k+1} = \frac{1}{N} \sum_{i=1}^N h(f(X_k^i))$$

The error covariance in the estimated observed output  $\hat{Y}_{k+1}$  is,

$$Y_{cov} = R + \frac{1}{N} \sum_{i=1}^N \left[ (h(f(X_k^i)) - \hat{Y}_{k+1})(h(f(X_k^i)) - \hat{Y}_{k+1})^T \right]$$

The cross-covariance between X and Y is,

$$XY_{cov} = \frac{1}{N} \sum_{i=1}^N \left[ (f(X_k^i) - \hat{X}(-)_{k+1})(h(f(X_k^i)) - \hat{Y}_{k+1})^T \right]$$

The Kalman Gain K, is given by,

$$K_{k+1} = \frac{XY_{cov}}{Y_{cov}}$$

Once we obtain the actual measurement for the  $(k + 1)^{th}$  step denoted by  $Y_{k+1}$ , we can write the update equations as follows:

The post-measurement *a posteriori* mean is given by,

$$\hat{X}(+)_{k+1} = \hat{X}(-)_{k+1} + K_{k+1}[Y_{k+1} - \hat{Y}_{k+1}]$$

And, the *a posteriori* error covariance by,

$$P(+)_k = P(-)_k - K_{k+1}Y_{cov}K_{k+1}^T$$

The Monte-Carlo Kalman Filter is an intuitive example to grasp the concept of the Statistical Linearized Kalman Filter, as well as understand our transition to Sigma Point Kalman Filters (which is explained in the following chapter). However, it is not a very practical

filter and is rarely (if at all) used in real world scenarios. This is due to fact that it requires knowledge of the prior pdf of  $X$ , the number of samples it demands for proper functioning is very high and the fact that if one uses these many samples one may as well go with the Particle Filter which is multi-modal compared to the unimodal of the MCFK.

## Chapter 4: State Estimation using the UKF

### 4.1 Introduction to the Sigma Point Approach

The Unscented Kalman Filter introduced by Julier, Simon J. and Uhlmann, Jeffrey K.[8] led the way for the family of Sigma Point Kalman Filters (which now include the UKF, scaled UKF, iterated UKF, Central-Difference Kalman Filter(CDKF) and some more). Thus, we introduce the concept of the sigma point approach with the Unscented Transform in mind. Every invention/discovery is based off an early intuition or gut feeling so to speak. The primal intuition that led to the discovery of the unscented transform is as follows: it is easier to approximate a Gaussian distribution than it is to approximate an arbitrary nonlinear function or transformation[9]. To further illustrate the unscented transform we consider an example below.

Let our main state vector be described by a random variable  $x$  having a distinct pdf. Assume a set of sigma points chosen from this distribution of  $x$ , whose mean is denoted by  $\hat{x}$  and the covariance by  $P_{xx}$ . These sigma points are in concept similar to the samples that are drawn from the prior distribution of  $x$ , as shown in the Monte-Carlo Kalman Filter (here is a link to that page 24). However, while they look extremely similar there is a key difference separating these samples from that in the MCKF, which will be subsequently discovered. If we apply a nonlinear transformation to these sigma points the resulting new distribution will not retain the same properties as that of  $x$ , which is a well established fact. Let the nonlinear function transform our RV  $x$  into another RV  $y$ .

$$y = f(x)$$

The prime objective here is to obtain the statistics of the RV  $y$ , its mean  $\hat{y}$  and covariance  $P_{yy}$ . We do this by transforming each of our sigma points drawn deterministically from  $x$ , through the nonlinear function  $f$ . This results in a set of transformed sigma points whose mean and covariance are now  $\hat{y}$  and  $P_{yy}$ . The calculation to find the mean and covariance is the similar<sup>1</sup> as that for the MCKF, described in equations are (3.3.2) for the mean and (3.3.3) for the covariance. The figure below delineates the process just conveyed.

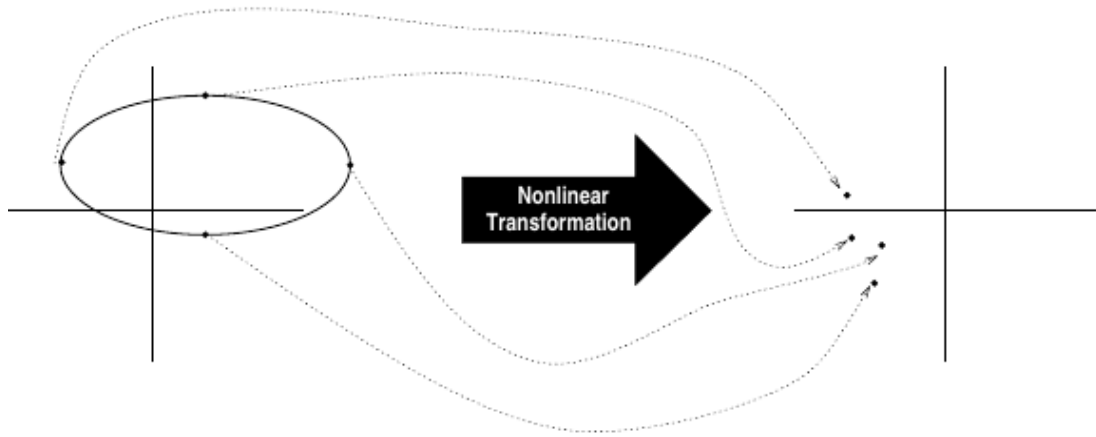


FIGURE 4.1: The transformation of sigma points through a nonlinear function[8]

I mentioned earlier that while the Sigma Point approach might seem to appear almost identical to the Monte-Carlo method, but it differs. The major differentiating fact is that in Monte-Carlo methods the samples are chosen from the *distribution* of the RV  $x$  and that too in a *random* manner. This would as require to have a distribution of  $x$  and a very large number of samples to successfully capture the properties of the distribution. However, the Sigma Point Filters select these points(samples) in a deterministic algorithm with weights attached to each sigma points. The different versions of the sigma point filters differ on how these weights are selected. All versions choose weights so that the method

<sup>1</sup>it is not exactly the same as we now have weights attached to each sigma point, thus it becomes a weighted average instead of a simple average

behaves perfectly for a Gaussian model (linear dynamics) and then optimize the weights for different criteria[7]. The plus point of any of these algorithms is that they can generate sigma points from just the first and second order moments of the distribution of  $x$ , i.e. its mean  $\hat{x}$  and covariance  $P_{xx}$  and do not require knowledge of the probability density function of  $x$ . Thus, one can see why this kind of a *black box* approach would be preferred in real life scenarios where knowledge about the state vector  $x$  in closed form solutions is not available to us.

## 4.2 The Unscented Transform

Coming to the selection scheme of the Unscented Transform, which is technically the entirety of the Unscented Transform. I use the original scheme outlined in Uhlmann's and Julier's first paper on the UKF[8].

The  $n$ -dimensional RV  $x$  with mean  $\hat{x}$  and covariance  $P_{xx}$  is approximated by  $2n + 1$  weighted points given by:

(note: There are a total of  $2 * n + 1$  weights one for each sigma point)

$$X_{sigma_0} = \hat{x} \qquad W_0 = \frac{\kappa}{n + \kappa} \quad (4.2.1a)$$

$$X_{sigma_i} = \hat{x} + \left( \sqrt{(n + \kappa)P_{xx}} \right)_i \qquad W_i = \frac{1}{2(n + \kappa)} \quad (4.2.1b)$$

$$X_{sigma_{i+n}} = \hat{x} - \left( \sqrt{(n + \kappa)P_{xx}} \right)_i \qquad W_{i+n} = \frac{1}{2(n + \kappa)} \quad (4.2.1c)$$

where  $\left( \sqrt{(n + \kappa)P_{xx}} \right)_i$  is the  $i^{th}$  row/column of the matrix square root of  $(n + \kappa)P_{xx}$  and

$W_i$  is the weight which is associated with the  $i^{th}$  sigma point and  $\kappa$  is the tuning factor which gives us extra room to fine tune the UKF to be application specific. Also, here  $n$  denotes the dimensionality of the state vector  $x$ . There also exist several articles on auto-tuning methods to tune these parameters of the UKF while performing on-line filtering and estimation, but we do not delve into these methods for the scope of my thesis.



A brief summary of the unscented transform is as follows:

1. Generate sigma points from the mean and covariance of the given RV using the weighted selection scheme mention in (4.2.1)
2. Pass each of these sigma points through the nonlinear function  $f$ , to obtain the point cloud of the transformed Sigma Points,

$$Y_{sigma_i} = f[X_{sigma_i}]$$

3. The mean of the transformed sigma points is given by the weighted averages of these points

$$\hat{Y} = \sum_{i=0}^{2n} W_i Y_{sigma_i}$$

4. The covariance is given by

$$P_{yy} = \sum_{i=0}^{2n} W_i [Y_{sigma_i} - \hat{Y}][Y_{sigma_i} - \hat{Y}]^T$$

### 4.3 The Scaled Unscented Transform

Simon Julier suggested a modified selection scheme for the selection of the sigma points in his papers on The Scaled Unscented Transformation[10]. This modification to the unscented transformation, helps increase the robustness of the sampling method against higher order nonlinearities beyond the second order[3].

This method uses adjustable scaling parameters  $(\alpha, \beta, \kappa)$  to allow for some fine tuning of the transform for specific applications. For notational ease we declare two more auxiliary parameters  $\lambda$  and  $\gamma$ . The structure of the scalar weights used in the unscented transform are as follows:

$$\lambda = \alpha^2(n + \kappa) - n \quad \text{Where } n \text{ is the dimension of the RV } x \quad (4.3.1a)$$

$$\gamma = \sqrt{n + \lambda} \quad (4.3.1b)$$

$$W_0^m = \frac{\lambda}{n + \lambda} \quad (4.3.1c)$$

$$W_0^c = \frac{\lambda}{n + \lambda} + (1 - \alpha^2 + \beta) \quad (4.3.1d)$$

$$W_i^c = W_i^m = \frac{1}{2(n + \lambda)} \quad \text{for } i = 1, 2, \dots, 2n + 1 \quad (4.3.1e)$$

As one can see we have two different sets of weights. The  $W_i^m$ 's are the weights used to calculate the mean of the transformed distribution and the  $W_i^c$ 's are the weights used to calculate the covariance of the transformed distribution. The selection scheme can be outlined as follows:

1. Generate sigma points from the mean and covariance of the given RV using the following weighted selection scheme:

$$X_{sigma_0} = \hat{x} \quad (4.3.2a)$$

$$X_{sigma_i} = \hat{x} + \left( \gamma \sqrt{P_{xx}} \right)_i \quad (4.3.2b)$$

$$X_{sigma_{i+n}} = \hat{x} - \left( \gamma \sqrt{P_{xx}} \right)_i \quad (4.3.2c)$$

2. Pass each of these sigma points through the nonlinear function  $f$ , to obtain the point cloud of the transformed Sigma Points,

$$Y_{sigma_i} = f[X_{sigma_i}]$$

3. The mean of the transformed sigma points is given by the weighted averages of these

points. The weight set used for this is  $W_i^m$ .

$$\hat{Y} = \sum_{i=0}^{2n} W_i^m Y_{sigma_i} \quad (4.3.3)$$

4. The covariance is given by the following equation below. We use a different weight set, of  $W_i^c$  for this operation.

$$P_{yy} = \sum_{i=0}^{2n} W_i^c [Y_{sigma_i} - \hat{Y}][Y_{sigma_i} - \hat{Y}]^T$$

Essentially only the  $W_0^c$  is different and  $W_i^c = W_i^m$  are the same for all  $i \neq 0$ , thus the above equation can also be simplified to be,

$$P_{yy} = W_0^c [Y_{sigma_0} - \hat{Y}][Y_{sigma_0} - \hat{Y}]^T + \sum_{i=1}^{2n} W_i^m [Y_{sigma_i} - \hat{Y}][Y_{sigma_i} - \hat{Y}]^T \quad (4.3.4)$$

## 4.4 Tuning the Weights

Here we discuss importance of the tuning factors (sometimes also referred to as the "twiddle factors") associated with the different weights of the Scaled Unscented Transform selection scheme. As the scaled version is much more elaborate, an overview on the selection of its weights will provide an insight into the non-scaled version too.

Referring to (4.3.1), we have the tuning parameters:  $\alpha, \beta, \kappa$ . The role they play in the transform and the probable range of values that they take on is explained as follows:

**Alpha ( $\alpha$ )** is the main scaling factor. It is used to limit/increase the acceptable region from which samples can be drawn about the mean. A smaller value of  $\alpha$  moves the sigma points towards the mean and vice-versa. The acceptable range is  $10^{-4}$  to 1. As  $\alpha \rightarrow 0$ , the influence of nonlinearities beyond the second order in the  $f(\cdot)$  on

the approximated mean and covariance is theoretically reduced[3]. When  $\alpha = 1$ , the scaled unscented transform is the same as the normal unscented transform.

**Beta** ( $\beta$ ) is used to incorporate prior knowledge of the distribution of  $x$ . For Gaussian distributions we usually set it to 2 (optimal)[11].

**Kappa** ( $\kappa$ ) is just a secondary scaling parameter. We usually set it to 0 for state estimation [11]. When  $\kappa = 0$  the  $X_{sigma_0}$  point is effectively omitted from the calculations of the mean and covariance calculations. Putting a negative value in  $\kappa$  might affect the positive semi-definiteness of the transformed covariance[3].

## 4.5 The UKF Algorithm

There are two versions of the Unscented Kalman Filter, the augmented and the non-augmented. I illustrate the use of the non-scaled unscented transform in each of the filters below for reasons of simplicity and ease of understanding the algorithm. Once, the central theme of the UKF is grasped, one can use either the scaled or the unscaled transform depending on what the application demands.

### 4.5.1 Augmented UKF

Its name is augmented because we need to augment the state vector to include the process disturbance. Thus, the dimensionality of the augmented state vector  $x^a$  becomes  $n^a = n + q$  where  $q$  is dimension of the process disturbance variance  $Q$ . Thus,

$$\hat{x}_k^a = \begin{bmatrix} \hat{x}_k \\ 0_{qx1} \end{bmatrix}$$

we also include the process disturbance variance in our main error covariance matrix  $P_{xx}$  augmenting it to,

$$P_{xx_k}^a = \begin{bmatrix} P_{xx_k} & 0_{nxq} \\ 0_{qxn} & Q \end{bmatrix}$$

Now, we begin the UKF:

1. The set of  $2n^a + 1$  Sigma Points are created by employing the selection scheme mentioned in (4.2.1) to the augmented state mean  $\hat{x}_k^a$  and covariance  $P_{xx}^a$

$$X_{k_0}^a = \hat{x}_k^a \qquad W_0 = \frac{\kappa}{n^a + \kappa} \quad (4.5.1a)$$

$$X_{k_i}^a = \hat{x}_k^a + \left( \sqrt{(n^a + \kappa) P_{xx_k}^a} \right)_i \qquad W_i = \frac{1}{2(n^a + \kappa)} \quad (4.5.1b)$$

$$X_{k_{i+n^a}}^a = \hat{x}_k^a - \left( \sqrt{(n^a + \kappa) P_{xx_k}^a} \right)_i \qquad W_{i+n} = \frac{1}{2(n^a + \kappa)} \quad (4.5.1c)$$

Here the  $X_{k_i}^a$  denotation is used for the sigma points, as writing 'sigma' in each of them would make it very cumbersome to read.

2. Pass each point through the nonlinear function  $f$ , to obtain the transformed sigma points  $X(-)_{k+1_i}^a$

$$X(-)_{k+1_i}^a = f^a(X_{k_i}^a, u_k) \quad (4.5.2)$$

3. The *a priori*, indicated by the minus(-) sign, mean  $\hat{x}(-)_{k+1}^a$  is given by

$$\hat{x}(-)_{k+1}^a = \sum_{i=0}^{2n^a} W_i X(-)_{k+1_i}^a \quad (4.5.3)$$

4. And the *a priori* covariance  $P(-)_{xx_{k+1}}^a$  is computed as,

$$P(-)_{xx_{k+1}}^a = \sum_{i=0}^{2n^a} W_i [X(-)_{k+1_i}^a - \hat{x}(-)_{k+1}^a][X(-)_{k+1_i}^a - \hat{x}(-)_{k+1}^a]^T \quad (4.5.4)$$

5. Pass all these transformed sigma points through the observer function  $h$ , to obtain the Y sigma points  $Y_{k+1_i}$

$$Y_{k+1_i} = h(X(-)_{k+1_i}^a, u_k) \quad (4.5.5)$$

6. Compute the mean  $\hat{y}_{k+1}$  and covariance  $P_{yy_{k+1}}$  of these observer sigma points,

$$\hat{y}_{k+1} = \sum_{i=0}^{2n^a} W_i Y_{k+1_i} \quad (4.5.6a)$$

And since the observation noise is additive(especially in our case it is truly additive), we can just add the measurement noise variance  $R$  to  $P_{yy_{k+1}}$  to get the following,

$$P_{yy_{k+1}} = R + \sum_{i=0}^{2n^a} W_i [Y_{k+1_i} - \hat{y}_{k+1}][Y_{k+1_i} - \hat{y}_{k+1}]^T \quad (4.5.6b)$$

7. Calculate the Cross-Covariance between the X and Y sigma points

$$P_{xy} = \sum_{i=0}^{2n^a} W_i [X(-)_{k+1_i}^a - \hat{x}(-)_{k+1}^a][Y_{k+1_i} - \hat{y}_{k+1}]^T \quad (4.5.7)$$

8. The measurement update part of the UKF is the same as that for the MCKF (see the equations on page 25)

The Kalman Gain is given as,

$$K_{k+1} = \frac{P_{xy}}{P_{yy_{k+1}}} \quad (4.5.8a)$$

The *a posteriori* mean is given as,

$$\hat{x}(+)_{k+1}^a = \hat{x}^a(-)_{k+1} + K_{k+1}[y_{k+1} - \hat{y}_{k+1}] \quad (4.5.8b)$$

where  $y_{k+1}$  is the true measurement obtained at the  $k+1^{th}$  step. Also, this is the end of the filtering process block so need to extract the non-augmented state vector back again, thus

$$\hat{x}(+)_{k+1} = \hat{x}(+)_{k+1}^a[1 : n]$$

And, Finally the *a posteriori* covariance is given as,

$$P(+)_{xx_{k+1}} = P(-)_{xx_{k+1}} - K_{k+1}P_{yy_{k+1}}K_{k+1}^T \quad (4.5.8c)$$

Note: The reason why we augment the state vector, is to incorporate the effects of the process disturbance on the mean and covariance of the sigma points. This does mean that we have more sigma points to propagate, but it also means that the effect of the process disturbance are introduced with the same order of accuracy as the uncertainty in the state. Such an augmented scheme also implies that correlated noise sources can be implemented easily[8]. Also, one can extend this model in a similar fashion to incorporate the measurement noise inn the mean and covariance, if it is non-additive or incorporated in a nonlinear fashion in the observer (we do not do this since in our case for the mobile robots, we assume additive white Gaussian measurement noise). Thus, the augmented implementation is favoured when our process disturbance and/or measurement noise is introduced into the system in a nonlinear and/or non-additive way. Plus, unlike the EKF the UKF does not place any restrictions on the noise sources to be Gaussian RVs.

## 4.5.2 Non-augmented UKF

If we know that the process disturbance (and/or measurement noise) is additive in the state propagation then we do not need to augment the state vector and thus can reduce the dimensionality and number of our sigma points and save on some computational costs.

Since, not a lot is changed in the implementation, I will only outline the differences in the non-augmented UKF algorithm instead of rewriting it.

1. The Selection scheme remains the same as described in (4.2.1), as we do not tamper with  $\hat{x}_k$ ,  $P_{xx_k}$  or  $n$ .
2. Generate the sigma points and instantiate them through the nonlinear function  $f$  and obtain the mean of the transformed sigma points. However, when we are calculating the covariance of the transformed sigma points we add the process disturbance variance  $Q$  to it, altering (4.5.4) as follows,

$$P(-)_{xx_{k+1}} = Q + \sum_{i=0}^{2n} W_i [X(-)_{k+1_i} - \hat{x}(-)_{k+1}] [X(-)_{k+1_i} - \hat{x}(-)_{k+1}]^T \quad (4.5.9)$$

but because we just included the effects of the process disturbance in the error covariance, we need to redraw the sigma points again, to incorporate this effect in the sigma points. We do this by using the recently obtained mean  $\hat{X}(-)_{k+1}$  and covariance  $P(-)_{xx_{k+1}}$  in the selection scheme given by (4.2.1).

3. The rest of the procedure remains the same as in (4.5.1)

## 4.6 The Square Root UKF

The drawback of the UKF is its computational complexity and comparatively slow speed of operation (as to that of the EKF), thus despite its superior performance over the EKF it still is not used in applications that are constrained by low computational capabilities.



Thus, if we could find a way to increase the computational efficiency of the UKF while still maintaining its efficient filtering index, we will have on our hands an efficient and fast state estimator and online filtering tool. The Square Root UKF does just this.

Rudolph Van der Merwe and Eric Wan introduced the Square-Root Unscented Kalman Filter. The following reasoning and algorithm are taken from their paper on the same[11]. The most computationally expensive operation in the UKF corresponds to calculating the new set of sigma points at each time update. While  $\sqrt{P_{xx}}$  is an integral part of the UKF, it is still the full covariance  $P_{xx}$  which is recursively updated. In the SR-UKF implementation,  $S$ , which is the square root of  $P_{xx}$  will be propagated directly, avoiding the need to refactorize at each time step.

The Square Root form of the UKF use the following linear algebraic techniques:

**Qr Decomposition** The QR decomposition or factorization of a matrix  $A_{l*n}$  is given by

$A^T = QR$ , where  $Q_{n*n}$  is an orthogonal matrix and  $R_{n*l}$  and  $n \geq l$ . The upper right triangular part of  $R$ ,  $\tilde{R}$ , is the transpose of the Cholesky factor of  $P = AA^T$ . This culminates into  $\tilde{R} = S^T$ . The notation used for the QR decomposition operation of a matrix that just returns  $\tilde{R}$  is: `'qr{.}'`<sup>2</sup>.

**Cholesky Factor Updating** If  $S$  is the original Cholesky factor of  $P = AA^T$ , then the

Cholesky factor of the rank 1 update or downdate,  $P \pm \sqrt{v}uu^T$  is denoted as  $S = cholupdate\{S, u, \pm v\}$ . If  $u$  is a matrix and not a vector, then we simply perform the  $cholupdate\{S, col_i, \pm v\}$  consecutively, for  $i = 1 : M$  where  $M$  is the number of columns of the matrix  $u$  and  $col_i$  denotes the  $i^{th}$  column of  $u$ .

**Efficient Least Squares** The solution to the equation  $(AA^T)x = A^Tb$  also corresponds

to the solution of the overdetermined least squares problem  $Ax = b$ . This can be solved efficiently using a QR decomposition with pivoting (implemented in Matlab's `'/'` operator).

---

<sup>2</sup>For further inquiry as to what is the exact computational complexity of the operations described in the square root UKF refer to the source[11]

Before we start the algorithm, a note on why we are using the Cholesky factorization / decomposition method for the initial matrix square root:

If we have a positive semi-definite matrix  $P$ , then it can have many square roots. In addition to this for any real valued matrix  $S$  that satisfies the following equation,

$$P = SS^T$$

is a valid square root of  $P$ . Now, one of the forms of the Cholesky Decomposition of a matrix is,

$$A = R^T R$$

where  $R$  is an upper triangular matrix. Thus, we can use the Cholesky Decomposition of the covariance matrix as an alternative to its usual matrix square root. The advantage of this being added numerical efficiency and stability as the Cholesky factors of  $P$  are generally much better conditioned for matrix operations than  $P$  itself. The idea of using a Cholesky factor for covariance matrix was first implemented by James E. Potter in his efforts to improve the numerical stability of the measurement update equations. His implementation came to be called as *square-root filtering*.<sup>3</sup>

#### 4.6.1 The SR-UKF Filter Algorithm

1. Initialize with the initial estimate of the state vector to be  $\hat{X}_0$  and the initial error covariance to be  $P_0$ . Thus, forming the Cholesky factor of  $P_0$ ,

$$S_0 = cholP_0$$

Also, the weight values need to assigned at this point. For this algorithm I employ the scaled unscented transform scheme mentioned in 4.3.

---

<sup>3</sup>More details on this can be found in the chapter "Implementation Methods" in the book "Kalman Filtering: Theory and Practice using Matlab"[3]

2. We start with the cyclic process that is repeated at each iteration. The iteration being marked by  $k$  and the sigma points being denoted by the lowercase  $i$ .

Generate the sigma points using the Cholesky factor of the error covariance  $S(+)_k$ ,

$$X_{k_0} = \hat{x}(+)_k \quad (4.6.1a)$$

$$X_{k_i} = \hat{x}(+)_k + \gamma S_k \quad \text{for } i = 1, 2, \dots, n \quad (4.6.1b)$$

$$X_{k_{i+n}} = \hat{x}(+)_k + \gamma S_k \quad \text{for } i = n + 1, \dots, 2n \quad (4.6.1c)$$

$$(4.6.1d)$$

3. Instantiate each sigma point through the nonlinear function  $f$ ,

$$X(-)_{k+1_i} = f(X_{k_i}, u_k) \quad \text{for } i = 0, 1, \dots, 2n$$

4. Now forming the new mean and covariance of the transformed sigma points,

$$\hat{x}(-)_{k+1} = \sum_{i=0}^{2n} W_i^m X(-)_{k+1_i} \quad (4.6.2a)$$

The *a priori* time-update of the Cholesky factory of the error covariance is formed using the QR decomposition of the compound matrix containing the weighted sigma points from  $i = 1$  to  $i = 2n$

$$S(-)_{k+1} = qr\{[\sqrt{W_i^c}(X(-)_{k+1}|_{i=1:2n} - \hat{x}(-)_{k+1}) \quad \sqrt{Q}]\} \quad (4.6.2b)$$

Where the operation  $(X(-)_{k+1}|_{i=1:2n} - \hat{x}(-)_{k+1})$  implies subtraction of the mean from each of the sigma points.

A separate subsequent Cholesky update/downdate is necessary since the weight of the 0<sup>th</sup> sigma point  $W_0^c$  maybe negative

$$S(-)_{k+1} = cholupdate\{S(-)_{k+1}, X(-)_{k+1_0} - \hat{x}(-)_{k+1}, W_0^c\} \quad (4.6.2c)$$

5. Redraw the sigma points to incorporate the effect of the process disturnce in them, since we are using the non-augmented version of the UKF.
6. Instantiate each point through the observer function h,

$$Y_{k+1_i} = h(X(-)_{k+1_i}, u_k) \quad for \quad i = 0, 1, \dots, 2n$$

7. Find the mean and covariance of the now transformed  $Y_{k+i}$  sigma points in a similar fashion

$$\hat{y}_{k+1} = \sum_{i=0}^{2n} W_i^m Y_{k+1_i} \quad (4.6.3a)$$

$$S_{Y:k+1} = qr\{[\sqrt{W_i^c}(Y_{k+1}|_{i=1:2n} - \hat{y}_{k+1}) \quad \sqrt{R}]\} \quad (4.6.3b)$$

$$S_{Y:k+1} = cholupdate\{S_{Y:k+1}, Y_{k+1_0} - \hat{y}_{k+1}, W_0^c\} \quad (4.6.3c)$$

8. Finding the Cross-Covariance of X and Y sigma points and the Kalman Gain,

$$P_{xy} = \sum_{i=0}^{2n} W_i^c [X(-)_{k+1_i} - \hat{x}(-)_{k+1}] [Y_{k+1_i} - \hat{y}_{k+1}]^T \quad (4.6.4a)$$

Since the  $S_{Y:k+1}$  is a square and triangular matrix, efficient "back-substitutions" can be used to solve for the Kalman gain  $K_{k+1}$  directly without the need for a matrix inversion,

$$K_{k+1} = (P_{xy}/S_{Y:k+1}^T)/S_{Y:k+1} \quad (4.6.4b)$$

9. Finally, after getting the actual sensor measurements for the  $k + 1^{th}$  step,  $y_{k+1}$ , we make the *a posteriori* updates to the mean and the Cholesky factor of the error covariance,

$$\hat{x}(+)_{k+1} = \hat{x}(-)_{k+1} + K_{k+1}(y_{k+1} - \hat{y}_{k+1}) \quad (4.6.5a)$$

The *a posteriori* measurement update of the Cholesky factor of the state covariance is calculated by applying  $m$  sequential Cholesky downdates to  $S(-)_{k+1}$ , where  $m$  is the number of columns of the matrix  $K_{k+1}S_{Y:k+1}$ , and the downdate vectors are the columns of this matrix.

$$S(+)_k = cholupdate\{S(-)_k, K_{k+1}S_{Y:k+1}, -1\} \quad (4.6.5b)$$

Out of all the UKF implementation versions, the square-root UKF has better numerical properties and guarantees positive semi-definiteness of the underlying state covariance  $P_{xx}$ [11].

## 4.7 An Illustrative comparison of the UKF with the EKF

Now, that we learnt about the various flavours of the UKF, let us examine an illustration comparing estimation accuracy of the EKF and the UKF for the mean and error covariance of the state vector  $x$ , after it is transformed through a nonlinear function. To better gauge the performance of either of these filters, we juxtapose them with a Monte-Carlo Sampling Method(with a large number of samples), which can be taken as the ground value for the 'true' mean and error covariance of the state.

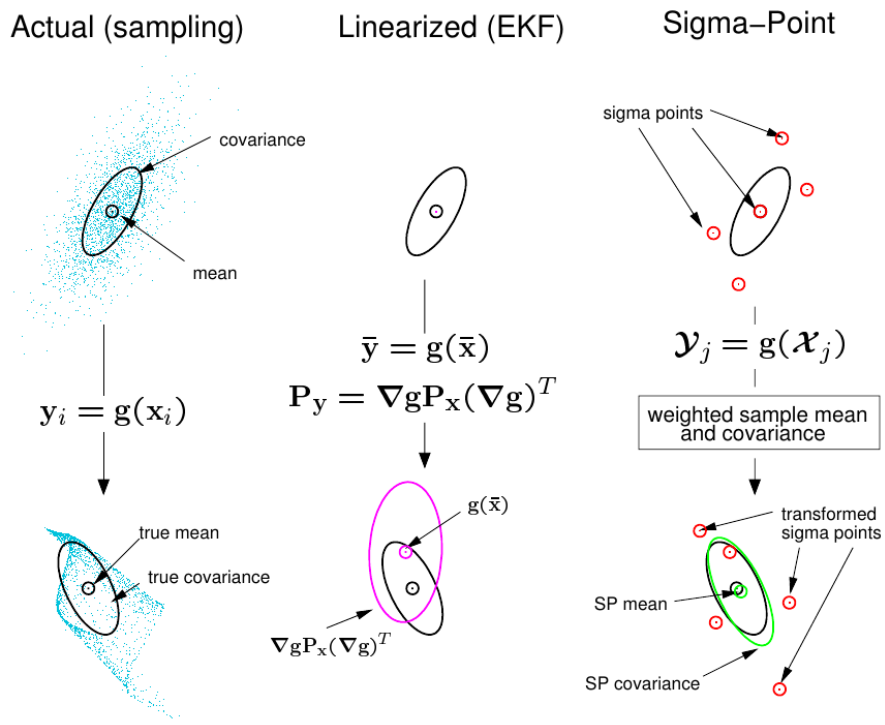


FIGURE 4.2: Comparison of mean and covariance sampling by Monte-Carlo Sampling, EKF and UKF[11]

## Chapter 5: Results: Simulation and Analysis

### 5.1 Matlab Simulation

Matlab is used for simulating my system and filter design. The reasons for choosing Matlab are:

1. Controls and Electrical engineering community favours it. Hence, many will find it easy to read and analyze my code, thereby relating to it.
2. Prototyping is very easy on Matlab. Thus one can concentrate more on the filter design rather than worry about its implementation.
3. It provides in-built support for Matrix Operations. The Kalman Filter relies heavily on Matrix Math, thus, it makes Matlab a convenient environment.
4. Excellent Plotting and Graphing support.

Matlab does have certain inefficiencies which makes it very slow when compared to other programming languages like C,C++,etc. However, all the filters are written in Matlab, thus evaluating them is still based on a fair comparison. One can switch to a C/C++ implementation when dealing with a real-time implementation of the Filter for a truly efficient and fast operation.

The codes used for the simulations and other verification schemes can be used to recreate any of the results and plots documented in the sections below. These are available upon request. If you intend to obtain them please drop a mail to [surajravi@gmail.com](mailto:surajravi@gmail.com) regarding the same.

### 5.1.1 Environment Variables

The various system parameters and constants that are used are as follows:

**Length**  $l$  is the length of the robot specified in meters. For all simulations it is set this to 2 meters. The length of the robot would in turn affect the radius of curvature, this is shown by the equation in (2.1.1).

$$l = 2m$$

**Gain** dictates the proportionality of the control law. Depending on the value set to gain we will make sharper turns (for a high value set to gain) or more gradual smoother turns (for a low value set to gain). One can try out different values of gain and set the one that gives the best results for the particular application at hand. For the entirety of the simulations, gain is set to 2.

$$Gain = 2$$

**Velocity**  $v$  is the velocity of the rear wheels of the robot. It is set to 1 meter per second for all the simulations.

$$v = 1 \text{ m/s}$$

**Discretization Time Interval**  $\delta t$  is the time step we use for our numerical integration method in seconds. It is set as follows:

$$\delta t = 0.1 \text{ s}$$

**Process Disturbance**  $Q$  is the variance of the process disturbance. As previously discussed, we have process disturbance only in our heading ( $\psi$ ) and not for any other state variable. Thus it is a scalar and it takes on the following value:

$$Q = 0.05^2;$$



**Measurement Noise**  $R$  is the variance of the measurement noise. For all the filters, I include measurement noise only in the x and y coordinate. It is absent from the  $\psi$  variable as  $\psi$  is not measured at all. The value of the  $R$  matrix is given below:

$$R = \begin{bmatrix} 0.2^2 & 0 \\ 0 & 0.2^2 \end{bmatrix}$$

**Initial Error Covariance**  $P_0$  is the value given by  $E[(\hat{X}_0 - X_0)(\hat{X}_0 - X_0)^T]$ . Here  $\hat{X}_0$  is the initial best guess of the state vector before beginning with the filtering operation.  $X_0$  is the true state vector (used for our simulations). Since we neither have knowledge of the PDF of the state vector  $X$  nor access to the true state vector  $X_0$ , we set this value arbitrarily. Trial and error methods are used to fine tune this value to increase the accuracy of the filter. The value used in all the simulations is given as:

$$P_0 = \begin{bmatrix} 0.2^2 & 0 & 0 \\ 0 & 0.2^2 & 0 \\ 0 & 0 & (\frac{\pi}{4.0})^2 \end{bmatrix}$$

A note about the Initial Estimate of the state vector  $\hat{X}_0$ : This can be set to a completely random value and allow the filter catch up to the true state at the expense of a certain number of iterations of the simulation. Some approaches even assume that they have exact knowledge of the initial conditions of the state, and set  $\hat{X}_0 = X_0$  and thus making  $P_0 = 0_{n \times n}$ . The approach used in this thesis sets  $\hat{X}_0$  to a value near the true state (by including some random noise over the value of the true state vector).

## 5.2 Graphs

Each of the filters are tested out on two different paths.

**Path 1** The first path is more straightforward and has a single destination in its entire course. However I make the observer function ( $h(\cdot)$ ) non-linear in the simulation for this path. This is done on purpose to facilitate a comparison of the all the filters with the IEKF, as the IEKF is only advantageous in the case of non-linearity in  $h(\cdot)$ .

The  $h(\cdot)$  I employ is specifically this:

$$Y = \begin{bmatrix} (\hat{x}_{co-ord} + \text{noise})^3 \\ (\hat{y}_{co-ord} + \text{noise})^3 \end{bmatrix}$$

Since there are high non-linearities in this simulation, please consider the resultant path plots and accuracy measures accordingly. There is a lot of noise present in them, hence the skewed plots.

**Path 2** The second path has a linear  $h(\cdot)$ , but, it has multiple destination (analogous to checkpoints) fed to it in a sequential manner. It first completes the entire path to the first checkpoint in the list and then once it has reached that destination (with a small room for error) it removes that checkpoint from the list and moves on to the next set of destination coordinates. The list of the destination coordinates is provided in the following manner:

$$X_{des} = \begin{bmatrix} x_{des1} & x_{des2} & \dots & x_{desp} \\ y_{des1} & y_{des2} & \dots & y_{desp} \end{bmatrix}$$

Here,  $p$  is the total number checkpoints in the list.

Note: The flavour of UKF used in the simulations and comparisons that are documented below is the Scaled Unscented Kalman Filter (non-augmented).

### 5.2.1 EKF Path 1

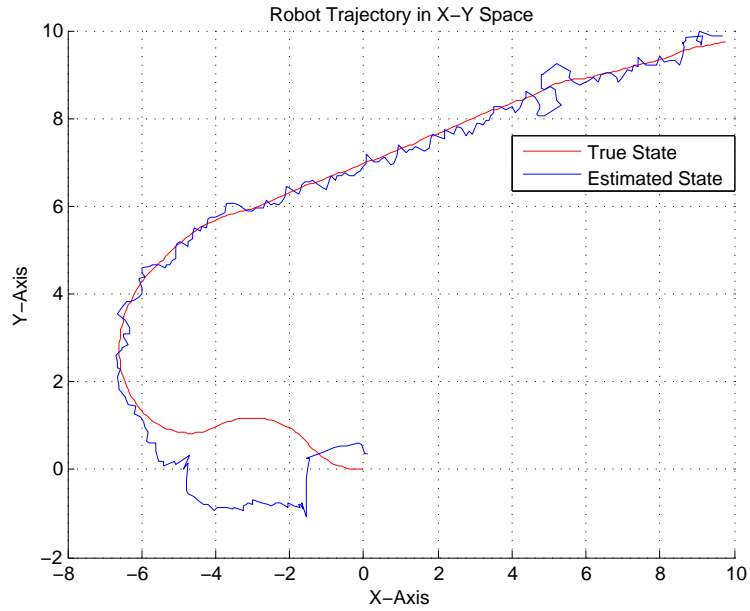


FIGURE 5.1: EKF Plot for True v/s Estimated Robot Trajectory

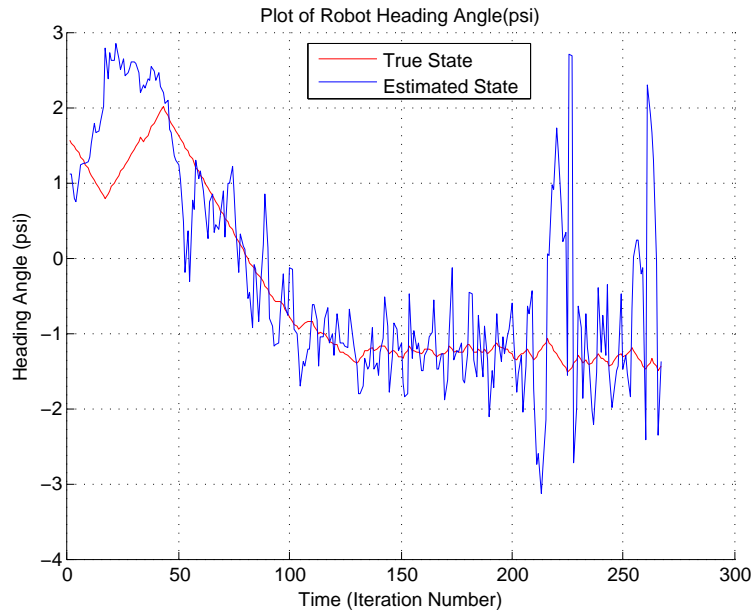


FIGURE 5.2: EKF Plot for True v/s Estimated Heading Angle

### 5.2.2 EKF Path 2

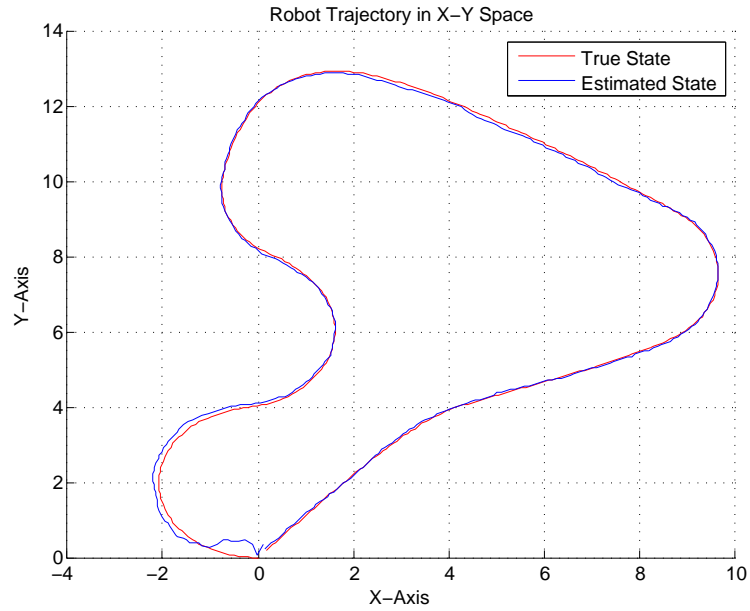


FIGURE 5.3: EKF Plot for True v/s Estimated Robot Trajectory

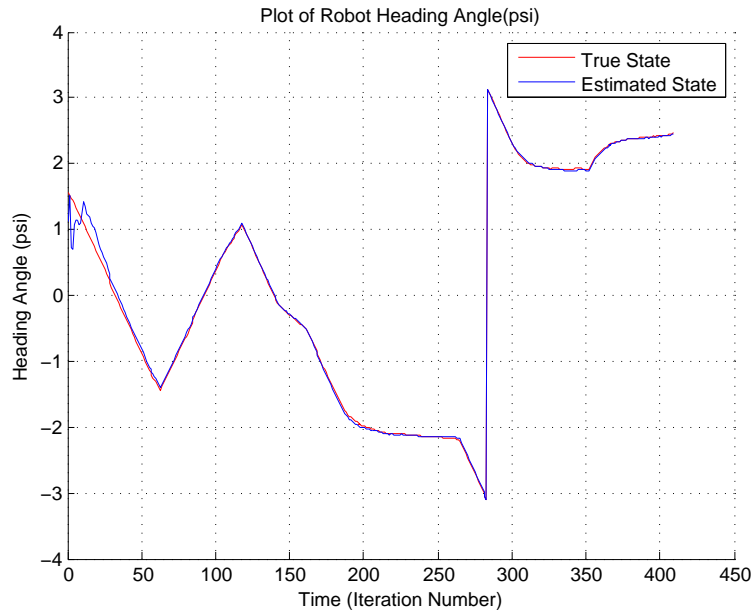


FIGURE 5.4: EKF Plot for True v/s Estimated heading Angle

### 5.2.3 IEKF Path 1

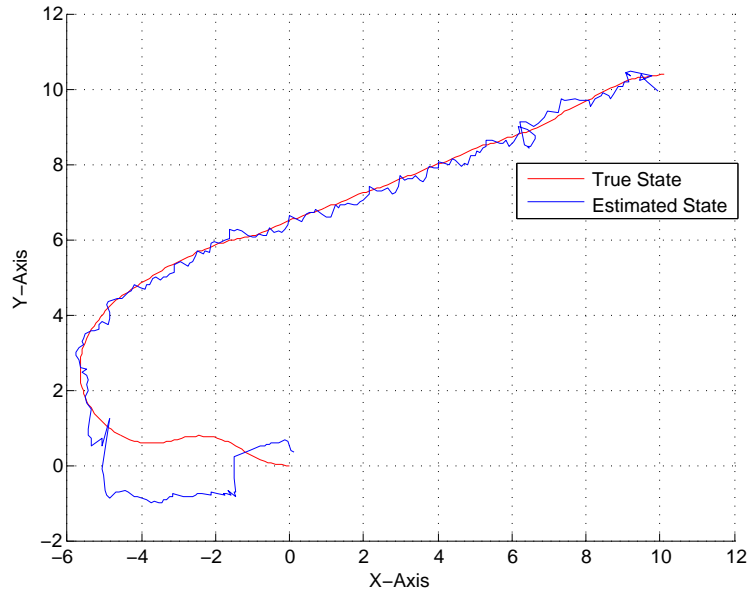


FIGURE 5.5: IEKF Plot for True v/s Estimated Robot Trajectory

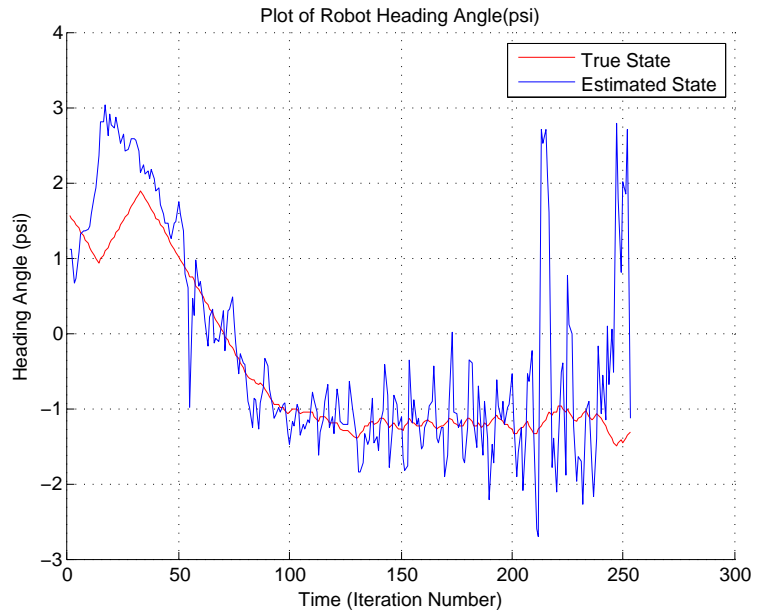


FIGURE 5.6: IEKF Plot for True v/s Estimated Heading Angle

### 5.2.4 IEKF Path 2

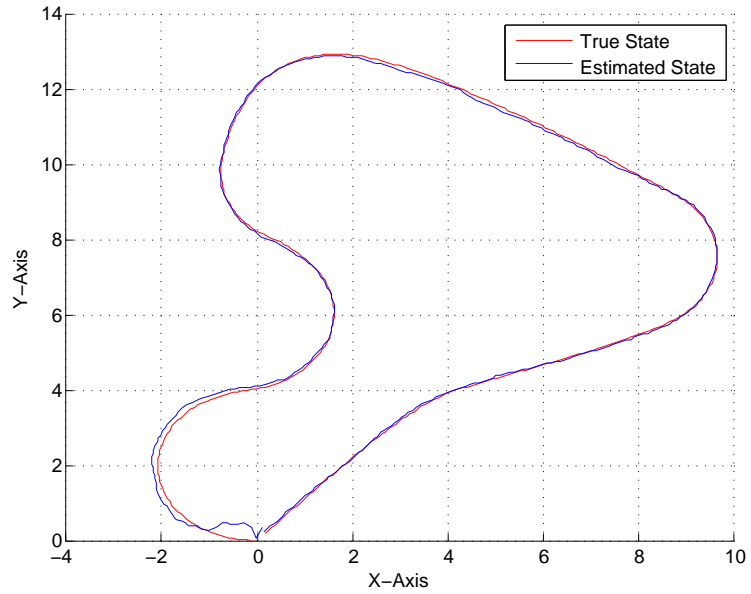


FIGURE 5.7: IEKF Plot for True v/s Estimated Robot Trajectory

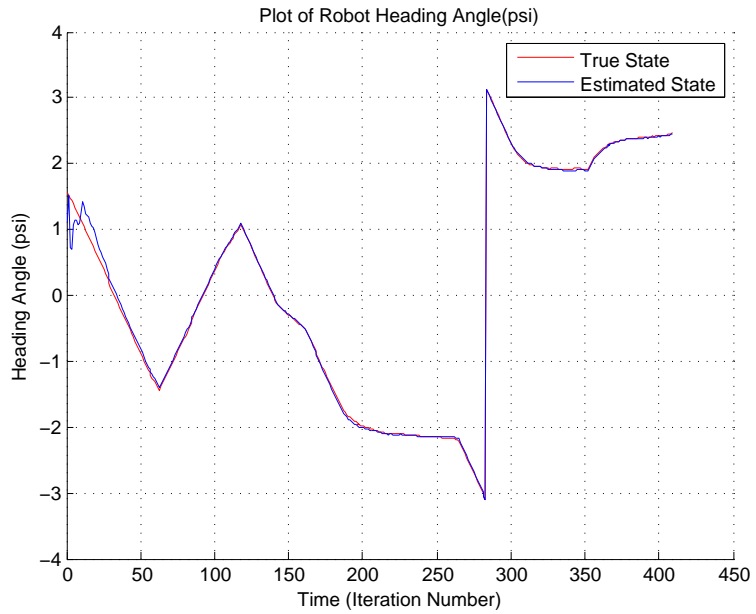


FIGURE 5.8: IEKF Plot for True v/s Estimated heading Angle

### 5.2.5 UKF Path 1

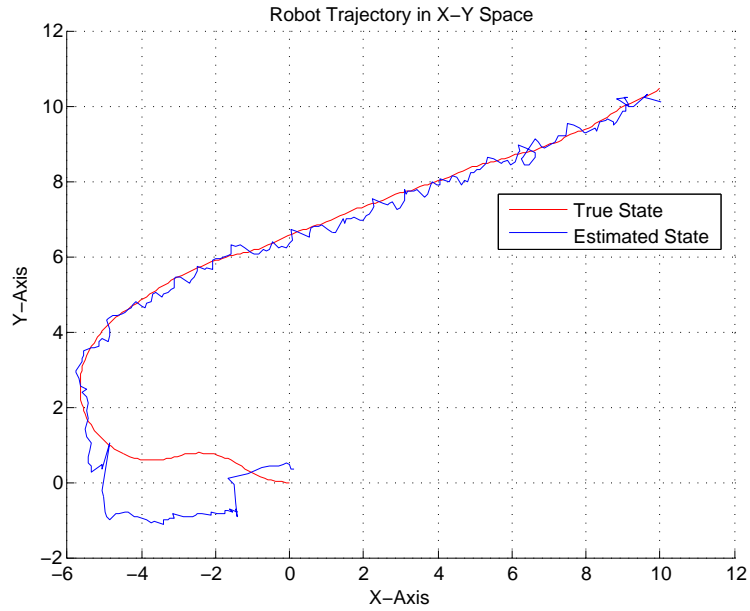


FIGURE 5.9: UKF Plot for True v/s Estimated Robot Trajectory

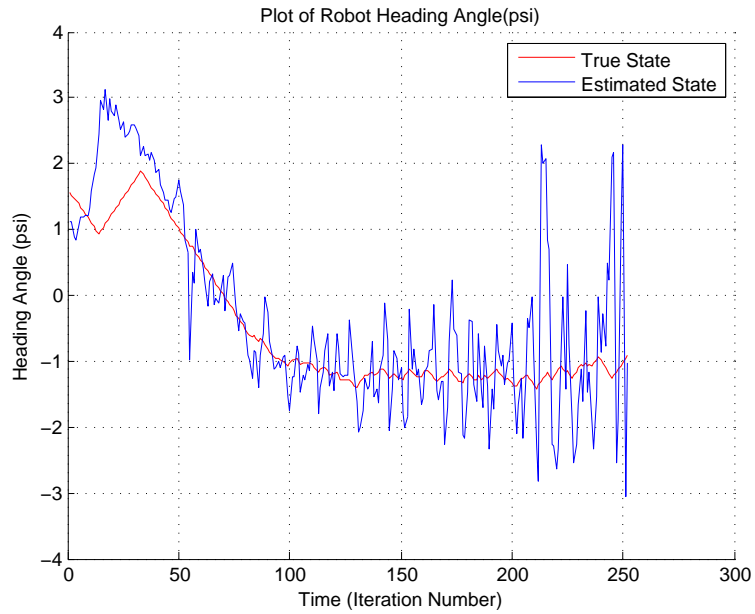


FIGURE 5.10: UKF Plot for True v/s Estimated Heading Angle

### 5.2.6 UKF Path 2

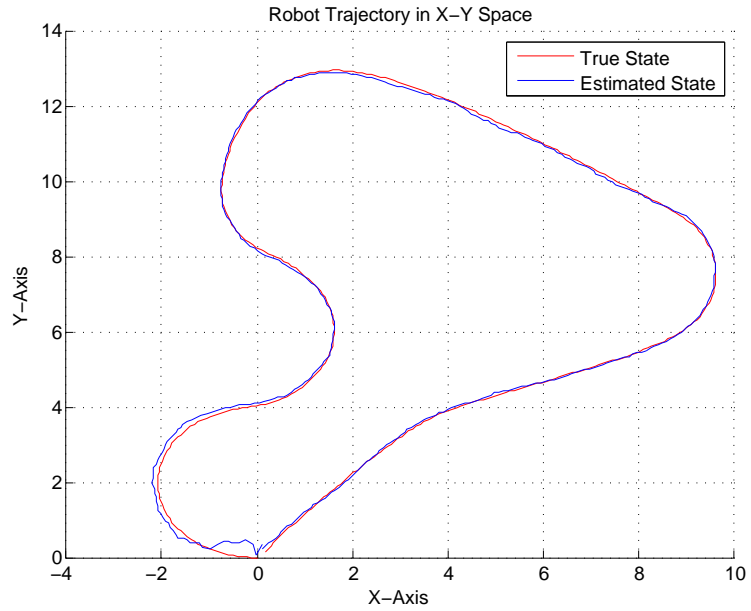


FIGURE 5.11: UKF Plot for True v/s Estimated Robot Trajectory

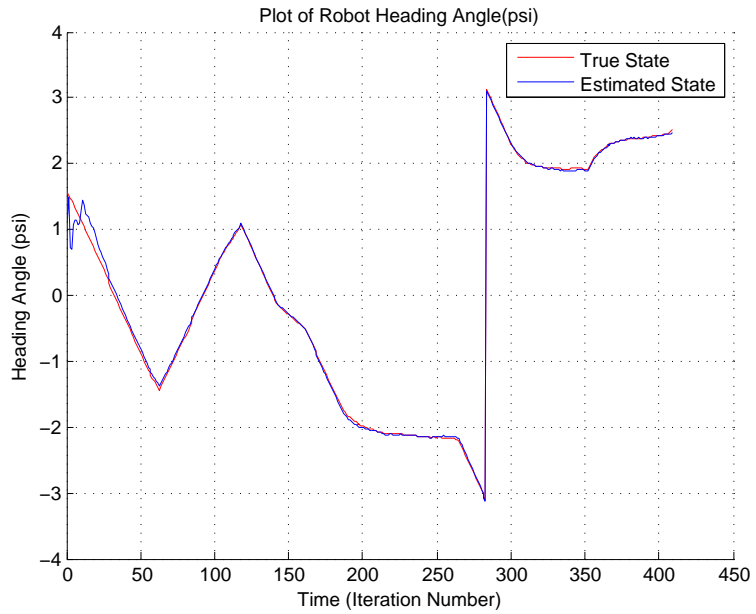


FIGURE 5.12: UKF Plot for True v/s Estimated heading Angle



### 5.2.7 Accuracy and Computational Costs (Time)

The accuracy of the filters is measured by calculating their Mean Squared Error (MSE) over the entire length of the simulation. Note that the MSE for x and y coordinates is calculated separately and that of the  $\psi$  is calculated separately as they have different units of measurement (meters and radians respectively).

Functions are made to carry out specific subroutines. This approach makes it possible to measure the time spent in each function and compare it for the various different filters. Matlab's 'Run and Time' feature enables this and gives the necessary numbers to facilitate a comparison between filters.

A list of the various functions used and their descriptions:

***stateprop*** this is where the system dynamics of the mobile robot are coded. The only function of *stateprop* is to propagate the state forward by 1 time step as per the specified dynamics.

***anglenormalization*** serves the function of keeping the angle values in the range of 0 to  $\pi$ . If this is not done regularly at every iteration and major alteration to the angles it might lead to a very unsrtable performance of the filter.

The tables below gives us a comparison of the filters with respect to accuracy and speed. The *stateprop* and *anglenorm* represent the time spent those functions respectively in seconds. All time is in seconds.

TABLE 5.1: Comparison Table for Path 1

Filters	MSE (x and y)	MSE $\psi$	Total Time	<i>stateprop</i>	<i>anglenorm</i>
EKF	0.5188	0.8391	0.183	0.008	0.017
IEKF	0.4206	0.8726	0.560	0.026	0.009
UKF	0.5001	0.7616	1.527	0.157	0.039

TABLE 5.2: Comparison Table for Path 2

Filters	MSE (x and y)	MSE $\psi$	Total Time	<i>stateprop</i>	<i>anglenorm</i>
EKF	0.0069	0.0063	0.225	0.009	0.009
IEKF	0.0069	0.0063	1.786	0.083	0.093
UKF	0.0063	0.0064	2.657	0.255	0.036

### 5.3 Verification of the UKF Implementation

Such below average performance of the UKF leads to the question that weather its implementation scheme is correct or not. This combined with the fact that every one in the controls industry believes that the UKF is superior to the EKF, led to the developments of verification schemes for the UKF.

#### 5.3.1 Testing the Unscented Transform

The Unscented Transform is at the heart of the UKF. The rest is just the filtering algorithm, where the possibility of error is thin. Thus, if we check the functioning of the Unscented Transform to be correct and as desired, we can actually state with authority that indeed for this specific case of Mobile Robot State Estimation it is better to stick to the EKF. There are basically two aspects that need to be verified with the Unscented Transform:

##### Proper Selection of the Sigma Points

The Sigma points chosen in the UKF (or any filter from the family of Sigma Point Kalman Filters) are chosen deterministically. This poses the question that on a meta-level what is the underlying scheme for selecting the sigma points in the Unscented Transform. Investigating this would also provide a much better understanding of the transform.

The sigma points are chosen along the principal axis of the ellipse of the uncertainty covariance. Since in our case the system dynamics are 3-dimensional the uncertainty covariance i.e.  $P_{xx}$  translates to an ellipsoid. So to really confirm if our sigma points are truly being mapped along the principal axis of this ellipsoid we need to first draw this ellipsoid.

Now, to grasp the concept of this ellipsoid we need to consider another fact. There is a confidence region boundary that we need to stick inside. This is because our State vector Random Variable to be Gaussian in nature, and as such Gaussian Region of convergence spread till infinity. Thus as a practical measure we restrict this boundary to include 'almost all' area under the ellipsoid but not all, since as we progress further and further away from the mean the probability of the state vector residing in that space reduces drastically. For the particular verification scheme being implemented, the confidence region is set to 65%<sup>1</sup>.

The following steps are based of the knowledge I accumulated after reading a the following articles[12] [13].

1. Scale covariance matrix ( $P_{xx}$ ) with the Mahalanobis Distance. The Mahalanobis distance is given by the following Matlab command:

```
mahalanobis_distance = chi2inv(conf, dim);
```

where 'conf' is the confidence region as mentioned above and 'dim' is the dimension of the state vector (which in our case is 3).

2. Obtain the Eigen Values and Eigen Vectors of the Covariance Matrix

```
[V,D] = eig(P);
% Make sure that all our eigen values and vectors are real & non-negative
V = real(V);
D= real(D);
D = abs(D);
% Sorting the Eigen vectors by their eigenvalues in a decending order
[D order] = sort(diag(D), 'descend');
D = diag(D);
V = V(:, order);
```

---

<sup>1</sup>This value was attained empirically

### 3. Generate the points for a generic sphere

```
[X,Y,Z] = sphere(num);
```

### 4. Now we conform these generated sphere points to the surface of our Ellipsoid

```
L= sqrt(diag(D));  
w = (V*sqrt(D))* [X(:)'; Y(:)'; Z(:)'];  
z = repmat(Mu(:), [1 (num + 1)^2]) + w;
```

here 'Mu' is the mean of our State Vector ( $X$ ) around which the ellipsoid is centered.

### 5. Now just plot these generated points

```
holding = ishold;  
axis equal  
rotate3d on;  
shading flat  
s = mesh(reshape(z(1, :), [(num + 1) (num + 1)]), ...  
         reshape(z(2, :), [(num + 1) (num + 1)]), ...  
         reshape(z(3, :), [(num + 1) (num + 1)]));  
set(s, 'EdgeColor', [0,0,0], 'EdgeAlpha', 0.05, 'FaceColor', 'none');  
% The line below allows me to exclude the sphere itself from the legend  
set(get(get(s, 'Annotation'), 'LegendInformation'), 'IconDisplayStyle', 'off');
```

### 6. Plotting the Principal Axis of the Ellipsoid

```
% First the x-axis  
h = plot3([Mu(1); Mu(1) + L(1) * V(1, 1); Mu(1) - L(1) * V(1, 1)], ...  
         [Mu(2); Mu(2) + L(1) * V(2, 1); Mu(2) - L(1) * V(2, 1)], ...  
         [Mu(3); Mu(3) + L(1) * V(3, 1); Mu(3) - L(1) * V(3, 1)], ...  
         'Color', 'blue');
```

```

% Now the y-axis
h=[h;plot3([Mu(1); Mu(1) + L(2) * V(1, 2); Mu(1) - L(2) * V(1, 2)], ...
           [Mu(2); Mu(2) + L(2) * V(2, 2); Mu(2) - L(2) * V(2, 2)], ...
           [Mu(3); Mu(3) + L(2) * V(3, 2); Mu(3) - L(2) * V(3, 2)], ...
           'Color','black')];

% And finally the si-axis (this is the z-axis)
h = [h; plot3([Mu(1); Mu(1) + L(3) * V(1, 3); Mu(1) - L(3) * V(1, 3)], ...
             [Mu(2); Mu(2) + L(3) * V(2, 3); Mu(2) - L(3) * V(2, 3)], ...
             [Mu(3); Mu(3) + L(3) * V(3, 3); Mu(3) - L(3) * V(3, 3)], ...
             'Color','red')];

```

With this done we can now plot an instance of the generated sigma points to check if they truly lie on the Principal Axes.

The first plot is done with the value of  $\alpha = 0.5$ , as discussed in (4.3.1)  $\alpha$  is the spread of the sigma points about the mean.

As we can infer from the above figure 5.13, the spread of the sigma points about the mean is symmetric. There are two equidistant sigma points on either side of the mean on each of the principal axes of the ellipsoid. The distance of these sigma points from the mean is the same for all the  $2 * n + 1$  points (where  $n$  is the dimension of the state vector). As for verifying the proper functioning of alpha, we can tweak it around a bit and plot the spread again. The figure below shows the sigma points on the error ellipsoid when  $\alpha = 0.9^2$ .

Thus, we can now conclude without a doubt that the sigma point selection scheme is working as intended.

## Testing the Convergence of the Unscented Transform

The Unscented Transform (or Scaled Unscented Transform) should be convergent for our filter to maintain stability and not loose track of the state being estimated. There exists a very simple scheme to perform this verification. It is as follows:

---

<sup>2</sup>The larger the value of  $\alpha$  the farther away from the mean the sigma points will spread.

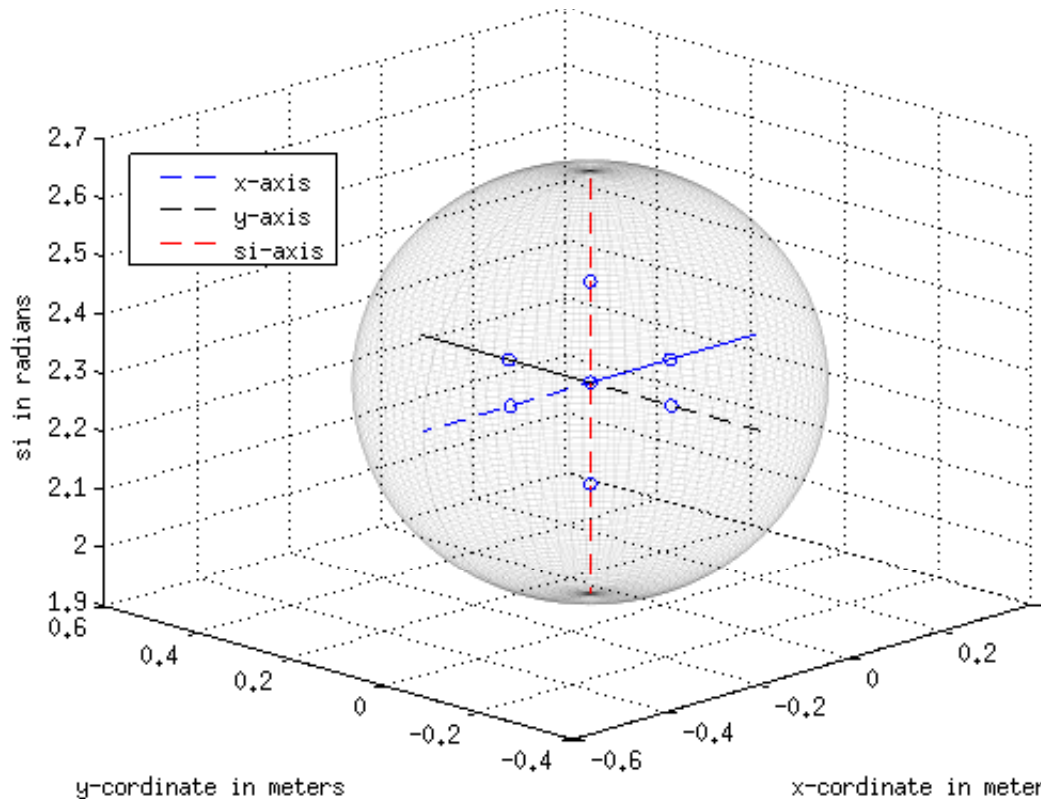


FIGURE 5.13: Error Covariance Ellipsoid: Sigma points around the mean with  $\alpha = 0.5$

1. With the initial Data given (i.e.  $P_{xx}, \alpha, \beta, \gamma, W^m$  &  $W^c$  and the mean  $\hat{X}$ ) generate set of sigma points as per the equations in (4.3.2).
2. We then pass these points through an identity transform, which basically means we do not touch these points at all.
3. Next we generate the mean and covariance of the transformed sigma points as described in (4.3.3) and (4.3.4) respectively.
4. Since we passed our sigma points through an identity transform, the state of the system should remain the same. Thus, the mean and covariance generated in the step above should match with the ones we started off with in the first place. If this does not hold then the Unscented Transform will be divergent and all will fail.

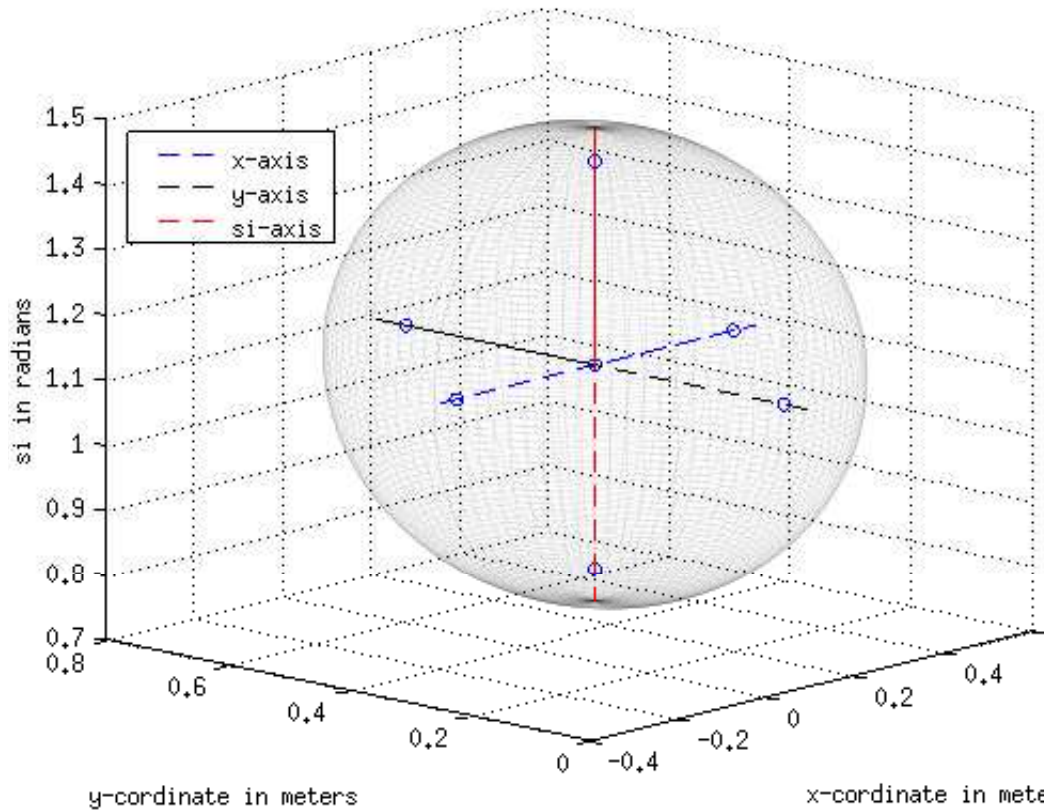


FIGURE 5.14: Error Covariance Ellipsoid: Sigma points around the mean with  $\alpha = 0.9$

A code snippet was written in Matlab for executing this verification scheme. Before the identity transform the mean and covariance were:

```
Pplus =
    0.0400    0    0
    0    0.0400    0
    0    0    0.6169
```

```
Xest =
    0.1212
    0.1081
```

1.2818

And after the identity transform the calculated statistics were:

Xest\_ident =

0.1212

0.1081

1.2818

Pminus\_ident =

0.0400    0.0000    -0.0000

0.0000    0.0400    -0.0000

-0.0000    -0.0000    0.6169

As one can see the mean remains unaltered. AS for the covariance, the misplaced  $-$  signs arise due to round-off errors and other computational errors. But these too are after the fourth decimal place, thus it is safe to conclude that are transform is actually convergent and working properly.

## 5.4 Averaging over multiple runs

One possible explanation to the current scenario of results would be the random noise induced into the system via process disturbance and measurement noise. Since these vary from run to run<sup>3</sup> it is always considered a good practice to average any Meas Square Error(MSE) over a good number of runs so that we eliminate the dependence of the results on randomness.

For our case at hand, we will compare just the EKF and the scaled UKF (non-augmented) over a thousand runs as this would allows us a more in-depth analysis of what the true MSE of each of them in the long run might be. To play it safe, the MSEs of each of the filters were averaged out over 1000 different runs (which means thousand different sets of random noise values).Path 2, as mentioned in the Graphs section above (Sec. 5.2), was used for

---

<sup>3</sup>The were still the same sets used to compare the filters in the sections above



these runs. The results obtained are shown in the table below.

TABLE 5.3: EKF v/s UKF MSE averaged over 1000 runs

Filter	MSE (x and y)	MSE $\psi$
EKF	0.0038	0.0412
UKF	0.0039	0.0400

## 5.5 Inference

The current claim in the Controls Community is that the UKF outperforms the EKF for non-linear applications and does just as well for linear applications. While this is true for the various non-linear systems that the UKF has been applied to, the results specific just to the case of Mobile Robot State Estimation are quite the contrary. This might be a case of the peculiar system dynamics of the Mobile Robot which causes this.

Thus, by far the best method for Mobile Robot State Estimation still remains to be the Extended Kalman Filter. In cases, when the noise level is too high the Iterated Extended Kalman Filter should be employed if the computational costs can be entertained.

The final conclusive finding of my comparison would be that the Extended Kalman Filter, is by far the best method for Mobile Robot State Estimation, within the realm of Gaussian Filters. Even outside the field of Gaussian Filters it is still the alternative with the highest accuracy to computational cost ratio.

## 5.6 Future Scope

The following are some extensions that could be built upon the work and analysis done in this thesis:

- Theoretical Investigation of why the UKF performs below par for the Mobile Robot problem.

- A mathematical proof of concept as to why the UKF does not give higher accuracy than the EKF for the Mobile Robot State Estimation.
- A possible change in the UKF particularly tailored for the current system dynamics filtering.

## Bibliography

- [1] Rudolf Kalman. A new approach to linear filtering and prediction problems. *Transactions of the ASME, Journal of Basic Engineering*, 82:35–45, 1960.
- [2] Greg Welch and Gary Bishop. An introduction to the kalman filter.
- [3] Mohinder S. Grewal and Angus P. Andrews. *Kalman Filtering Theory and Practice Using Matlab*. 3<sup>rd</sup> edition, September 2008. ISBN 9780470173664. URL <http://www.wiley.com/WileyCDA/WileyTitle/productCd-0470173661.html>.
- [4] Particle filter wikipedia page. URL [http://en.wikipedia.org/wiki/Particle\\_filter](http://en.wikipedia.org/wiki/Particle_filter).
- [5] Gerald Cook. *MOBILE ROBOTS: Navigation, Control and Remote Sensing*. Wiley-IEEE Press, June 2011. ISBN 9780470630211. URL <http://www.wiley.com/WileyCDA/WileyTitle/productCd-0470630213.html>.
- [6] Arthur Gelb, Joseph F. Kasper, Raymond A. Nash, Charles F. Price, and Arthur A. Sutherland. *Applied Optimal Estimation*. MIT Press, Cambridge, MA, 1974. ISBN 9780262570480.
- [7] Drew Bagnell and Keheng Zhang. Statistical techniques in robotics: Lecture on kalman filtering(part 2). CS lecture series in Carnegie Mellon University.
- [8] S.J. Julier and J.K. Uhlmann. A new extension of the kalman filter to nonlinear systems. In *11th International Symposium on Aerospace/Defense Sensing (AeroSense), Simulations and Controls*, 1997.

- [9] Simultaneous map building and localization for real time applications.
- [10] Simon J. Julier and Idak Industries. The scaled unscented transformation. In *in Proc. IEEE Amer. Control Conf*, pages 4555–4559, 2002.
- [11] Rudolph van der Merwe and Eric A. Wan. The square-root unscented kalman filter for state and parameter-estimation. URL <http://ece.ut.ac.ir/Classpages/S87/ECE150/Papers/Kalman-Filter/merwe01a.pdf>. Oregon Graduate Institute of Science and Technology.
- [12] Ellipse around the data in matlab – stackoverflow, . URL <http://stackoverflow.com/questions/3417028/ellipse-around-the-data-in-matlab>.
- [13] Error ellipse plot matlab code, . URL <http://openslam.informatik.uni-freiburg.de/data/svn/tjtf/trunk/matlab/plotcov2.m>.

## Curriculum Vitae

Suraj Ravichandran was born in the city of Mumbai, India. He completed his Bachelor of Engineering in Electronics and Telecommunication from the Thadomal Shahahni College of Engineering (Mumbai University). His research interests are Controls, Robotics and Artificial Intelligence. He is currently pursuing his Masters in Electrical Engineering in George Mason University.